

R. & M. No. 3596



MINISTRY OF TECHNOLOGY

AERONAUTICAL RESEARCH COUNCIL
REPORTS AND MEMORANDA

Oscillatory Pressure Measurements on a Flexible Slender-Wing Model at Low Subsonic Speeds

By F. Ruddlesden, D. A. Drane and P. W. Slaven
Structures Dept., R.A.E., Farnborough

LONDON: HER MAJESTY'S STATIONERY OFFICE

1969

PRICE 18s. 6d. NET

ROYAL AIRCRAFT ESTABLISHMENT
BEDFORD

Oscillatory Pressure Measurements on a Flexible Slender-Wing Model at Low Subsonic Speeds

By F. Ruddlesden, D. A. Drane and P. W. Slaven

Structures Dept., R.A.E., Farnborough

*Reports and Memoranda No. 3596**
December, 1967

Summary

Oscillatory pressure measurements have been made on a flexible slender-wing model in a low subsonic speed wind tunnel. The model was vibrated at 5 Hz in a single longitudinal bending mode, and measurements were taken at wind speeds of 140, 180 and 220 ft/s (43, 55 and 67 m/s) from 24 pressure transducers installed in one half of the model. Corresponding values of oscillatory pressures were calculated for comparison with those measured. It is shown that over the broad area of the wing there is good agreement between theory and experiment within the range of frequency parameters investigated. Near the apex of the wing shortcomings inherent in the theory may account for the discrepancies observed between theory and experiment.

CONTENTS

1. Introduction
2. Apparatus
 - 2.1. Wind-tunnel
 - 2.2. Description of model
 - 2.2.1. Structural details of model
 - 2.2.2. Instrumentation of model
 - 2.3. Model support
 - 2.4. Excitation
 - 2.5. Recording equipment
3. Determination of Mode Shape
4. Pressure Transducers
 - 4.1. Description of transducers
 - 4.2. Calibration of transducers

*Replaces R.A.E. Technical Report 67 316—A.R.C. 30 401

CONTENTS—*continued*

5. Wind-Tunnel Tests
 - 5.1. Experimental method
 - 5.2. Results
6. Calculated Pressure Distribution
 - 6.1. Method
 - 6.2. Results of calculations
7. Discussion of Results
 - 7.1. Experimental results
 - 7.2. Calculated values of pressure
 - 7.3. Comparison of theory with experiment
8. Concluding Remarks

Acknowledgements

References

Appendix A Measurement of mode shape

Appendix B Determination of pressure-transducer characteristics

Tables 1 to 4

Illustrations—Figs. 1 to 20

Detachable Abstract Cards

1. *Introduction*

The prediction of aerodynamic forces is one of the more uncertain aspects of a flutter calculation, and there is need for wind-tunnel data against which theory can be checked. The direct measurement of aerodynamic forces on a model oscillating in a non-rigid mode is not easy, however, it is possible to derive the forces from measurements of the pressure distribution.

Wind-tunnel measurements of oscillatory pressures have been made by Laidlaw¹ who investigated pressures on a series of wings of differing plan-forms oscillating rigidly in heave and pitch; Bergh² has undertaken similar work on wing and T-tail models oscillating in rigid body modes. Molyneux and Ruddlesden³ developed a pressure transducer intended for use in low-speed wind-tunnels; some of these transducers were installed in a rectangular wing, and the pressure distribution measured when the wing was oscillated in rigid modes. Investigations have also been made into oscillatory pressure distributions generated by models deforming in non-rigid modes. At the Ames and Langley Research Center of the NASA, pressures have been measured on a rectangular wing constrained to deform in a spanwise bending mode⁴, and a trapezoidal wing deforming in a torsion mode⁵.

Because of the interest, at the R.A.E., in wings of slender planform, it was decided to obtain wind-tunnel data using a model of this shape in a non-rigid mode. The wing was constrained to flex inexorably in longitudinal bending. Pressure transducers based on the type described in Ref. 3 were developed to

suit the requirements of this experiment. Twenty-four of these transducers were installed in spanwise rows in the starboard half of the wing.

The mode of deformation was determined in still air at each of three amplitudes when the model was being excited at 5 Hz. The prescribed experiments were then carried out at wind speeds of 140, 180, and 220 ft/s, (43, 55, and 67 m/s), the oscillatory pressures and phase angles relative to the motion being measured at each of the three amplitudes. Before and after each wind-tunnel test the pressure transducers were dynamically calibrated.

The experimental results were compared with calculations based on the theoretical work of D. E. Davies⁶. It was found that there is good agreement between theory and experiment over the main area of the wing. Discrepancies between theory and experiment were observed near the apex of the wing; these may be accounted for by short-comings inherent in the theory when applied to planforms of this type.

2. Apparatus

2.1. Wind Tunnel

The tests were made in the R.A.E. 5 ft open jet low-speed wind tunnel.

2.2. Description of Model

The model had a modified slender delta-wing planform, chordwise length 42.75 in (1.086 m), span 23.8 in (0.604 m), apex angle 35° with parabolic curved tips and a control surface provided at the trailing edge. The geometry of the model and the positions of the pressure transducers are shown in Fig. 1. The aerofoil was of symmetrical biconvex section, having a thickness/chord ratio of 6 per cent. In spanwise elevation the cross-section was diamond shaped terminated by a 0.010 in (0.25 mm) radius at the leading edges. The control was locked in the neutral position throughout this experiment.

2.2.1. *Structural details of model.* The main structural member was a $\frac{1}{8}$ inch (3.18 mm) thick steel plate shaped to planform and appropriately tapered at leading and trailing edges. Transverse stiffeners were welded to the plate normal to the fore-and-aft centreline of the model, thus ensuring that the mode of deformation would be essentially chordwise bending. The aerodynamic profile was realised by encasing the main portion of the plate in moulded flexible polyurethane foam; because thin tapered sections of this material were impracticable, transition fillets of epoxy resin were used to maintain the profile near the tapered edges of the plate.

A narrow ribbon of coarse carborundum was glued near the leading edges to form a transition band.

The model was supported at three points through trunnion blocks inserted into the plate. The forward trunnion was on the fore-and-aft centreline 0.121 m from the apex, and the rear trunnions were 0.984 m from the apex and equi-distant 0.086 m either side of the centreline. Similar trunnions were provided at the forcing points which were 0.552 m from the apex and 0.086 m either side of the centreline. The support and forcing trunnions are shown in Figs. 1 and 2.

2.2.2. *Instrumentation of model.* Fig. 2 shows the instrumentation of the model before the polyurethane filler was applied. (The plate is shown supported above one half of the box mould into which the foam mixture was injected.) Four strain-gauge units were disposed along the fore-and-aft centreline of the plate as shown in Fig. 1. Each unit consisted of a complete Wheatstone bridge so that the output was proportional to the strain at the applicable station. The respective outputs were intended to give intimation of any change of the mode shape that may have occurred due to air loading. Any of the four bridges could be used to generate the motion reference signal. Twenty-four differential pressure transducers were attached to the plate as designated in Fig. 1, and the precise ordinates of the positions are included in Table 1. Short pipes connected the transducers with the upper and lower surfaces of the wing so that the quantity sensed was the pressure difference between the two surfaces.

2.3. Model Support

The model was supported in the wind tunnel using a system of steel tubes and bracing wires (see Fig. 3).

2.4. Excitation

The system of excitation is shown diagrammatically in Fig. 4 and the actual mechanism in Fig. 3.

The model was excited inexorably by a swash-plate mechanism that was driven by an electric motor. A horizontal rod transmitted the motion from the swash-plate rider to a forked bell-crank lever situated beneath the model. Two stiffened tubes connected the forked ends of the bell crank to the driving trunnions within the model. A cross-bar, fixed to the lower ends of the tubes, was connected to one end of a beam that was free to oscillate in the vertical plane. The beam was supported at its mid-point on a cross-spring bearing that was anchored to the floor. The wing and beam formed a composite oscillatory system and, by adding weights to the beam, the resonance frequency of the system could be varied. The system was tuned so that its resonance frequency coincided with that at which the model was being driven. By doing this a consistent sinusoidal motion was maintained. Throughout these tests the frequency of excitation was 5 Hz. A primary check on the frequency was made by means of an electro-mechanical tachometer coupled to the wing driving mechanism, whilst a more precise indication was available in the form of a Lissajous figure continuously displayed on an oscilloscope as a result of matching the signal given by a low-frequency oscillator with one derived from the motion.

Motion of the swash-plate connecting rod was monitored by means of strain gauges attached to a cantilever spring strip. One end of this was fixed to the floor and the other effectively pinned to the rod. A variable displacement pump could also be connected to the swash-plate connecting rod when required for use in the pressure-transducer calibration procedure.

2.5. Recording Equipment

A block diagram of the recording equipment is shown in Fig. 5. One of the strain-gauge signals from the model was used as a motion reference with which to compare each of the pressure-transducer signals in turn. The signals were respectively switched to two matched amplifiers, one of which handled the pressure-transducer output and the other the strain-gauge reference. The outputs of the amplifiers were then fed to a Muirhead Phase Meter which measured the modulus voltage of the pressure-transducer signal, and the relative phase angle. A twin-beam oscilloscope connected in parallel with the phase meter was used to monitor the outputs; this arrangement also allowed direct current measurement of voltage to be made.

3. Determination of Mode Shape

The mode of deformation was determined in still air conditions with the model rigged in the wind tunnel. A Wayne-Kerr Vibration Meter, in conjunction with a unique measuring head, was used to resolve the vertical movement of points distributed over the surface of the model. The mode shape was measured for each of the three amplitudes pertaining to the main experiments. These amplitudes were in the ratios 1:2:3, the smallest having a total displacement of 6.96 mm at the point of excitation. When reduced, the three mode shapes were identical within experimental error. The normalised mode shape along the centreline chord, and the associated Table of non-dimensional ordinates are given in Fig. 6. The equipment used for the measurements is illustrated in Fig. 7, and a detailed description of the method is contained in Appendix A.

4. Pressure Transducers

4.1. Description of Transducers

All the pressure transducers used during the experiment were designed, developed and manufactured at the R.A.E. They were basically similar to the transducers described in Ref. 3 but differed in having to satisfy much more stringent requirements. In Ref. 3 maximum pressures in the region of ± 30 lbf/ft² (1440 N/m²) were recorded, whereas in the tests described here the maximum peak pressures were only expected to be about $\pm 3\frac{1}{2}$ lbf/ft² (167 N/m²). In order to meet the new specification the original transducer was redesigned to improve stability and sensitivity. Fig. 8 shows cross-sections of the current standard and side entry type transducers. It will be seen that the core of each type is a bobbin of epoxy resin to which is cemented a cylindrical rubber diaphragm. A cap is fitted over the bobbin to form an

annular chamber around the outside of the diaphragm. Drillings in the cap and bobbin allow pressures to be fed to each respective side of the diaphragm, thus causing it to flex with changes in differential pressure. The pressure points on the wing are connected to the drillings by pipes orientated according to the installation requirements. On the diaphragm are wound two lengths of Karma 0-00055 in (0.014 mm) diameter resistance wire which form the two active arms of a Wheatstone bridge; two dummy arms made from similar wire are wound on the core of the bobbin. Each arm of the bridge has a nominal resistance of 1020 ohm. During the experiments the transducers were operated at 12 volt DC and the sensitivity was sufficient to permit pressures of $\pm 0.06 \text{ lbf/ft}^2$ (2.9 N/m^2) to be measured.

4.2. Calibration of Transducers

After installing the wing in the wind tunnel the pressure transducers were calibrated under static conditions. Subsequent routine calibrations required during the experiments were carried out dynamically using oscillatory pressures generated by the pump driven from the swash-plate exciter. Details of the calibration procedure are given in Appendix B. Calibrations were carried out immediately before and immediately after each sequence of pressure measurements.

5. Wind Tunnel Tests

5.1. Experimental Method

In order to determine if air loading had any significant effect on mode shape a comparison of the outputs from the strain gauges mounted on the plate was made under still air and wind-on conditions in the course of each test.

Measurements of the oscillatory pressures were made at airspeeds of 140, 180 and 220 ft/s (43, 55 and 67 m/s). At each airspeed the model was excited to the three amplitudes of vibration, and, at each amplitude the value of modulus voltage and the corresponding phase angle transmitted by each of the twenty-four pressure transducers was recorded in turn. Every test was repeated so that in all eighteen sets of measurements were obtained.

5.2. Results

The outputs of the strain gauges indicated that the mode shapes were effectively the same under still air and wind-on conditions. The slight random variation that appeared were ascribed to experimental error. The recorded signals from the pressure transducers were converted to the representative pressures and then reduced to a non-dimensional form to make them compatible with the values obtained by calculation. (Described in Section 6.)

The form of reduction was:

$$\bar{p} = \frac{p_m}{\rho V^2 q_{i0}} \quad (1)$$

and the components extracted by:

$$p_r = \bar{p} \cos \theta \quad (2)$$

$$p_i = \bar{p} \sin \theta \quad (3)$$

where p_m = Measured pressure modulus

\bar{p} = Non-dimensional pressure modulus

p_r = In-phase non-dimensional pressure

p_i = In-quadrature non-dimensional pressure

θ = Measured phase angle

ρ = Air density

V = Air speed

$$q_{i0} = \frac{\text{amplitude at point of maximum displacement}}{\text{length of centreline chord}}$$

The non-dimensional components of all the recorded measured pressures are contained in Tables 1, 2 and 3, which refer respectively to each frequency parameter, based on the centreline chord, at which

the measurements were made, viz. 0.5, 0.6 and 0.8. The maximum and minimum values obtained by experiment are also shown superimposed on the calculated pressure-distribution curves shown in Figs. 9 to 15 which will be discussed in Section 6.

6. Calculated Pressure Distribution

6.1. Method

The method used for calculating the oscillatory pressures acting on the wing was devised by D. E. Davies.⁶ It assumes a flat-plate wing which may be of arbitrary planform provided that it is symmetrical about the centreline, and that the leading and trailing edges do not have sharp discontinuities. The downwash equation is solved approximately using a collocation method, that is, one in which the downwash equation is satisfied exactly at finite number of points; the distribution over the wing is then obtained by interpolation. The associated programme is R.A.E. 263A and this was used for making the pressure calculations.

When committed to the planform, the collocation points assume a formation that is governed by the style of the arrangement chosen. The array is always of lines of points oriented along the chord, each line having the same number of points. The number of lines distributed along the semi-span, and the number of points per line, are separately subject to choice, thereby the formation of the collocation-point arrangement can be varied. In the computer programme the maximum total of collocation points permissible was forty per half-wing. In order to demonstrate the effect of collocation-point arrangement, it was decided to calculate the pressure distribution given by two arrangements of collocation points, one having five rows of eight points and the other eight rows of five points. Because the method assumes that there is no kink in the leading edge, when in fact there is a kink at the wing centreline, the computational programme rounds off the leading edge to a degree dependent upon the arrangement of the collocation points chosen. The closeness with which the model planform near the apex would be represented by each chosen arrangement was investigated by calculation.

6.2. Results of Calculations

Figs. 9 and 10 show respectively the calculated in-phase and in-quadrature pressure-distribution curves along the centreline chord for the two arrangements of collocation points discussed in Section 6.1.

Figs. 11, 12 and 13 show the calculated components of pressure along the spanwise stations normal to the model centreline; for these curves $M = 0.197, 0.161$ and 0.125 respectively, and the collocation arrangement was eight rows of points distributed along the semi-span with five points in each row. Fig. 14 shows similar curves when $M = 0.125$ and the collocation arrangement was five rows with eight points in each row. A comparison of calculated pressures obtained using both arrangements of collocation data when $M = 0.197$ is shown in Fig. 15. The calculated pressures pertaining to the points on the model at which pressure measurements were made are tabulated in Table 4; values for both collocation arrangements are included.

The two arrangements of collocation points resulted, within the programme, in two artificial leading-edge shapes near the apex; both shapes are shown diagrammatically in Figs. 9 and 10. It can be seen that the effects of the calculation procedure are to round off the apex and reduce the lengths of chord lines in the vicinity of, and including, the centreline chord. The foremost points in the centreline chord of the artificial leading edges are at 0.05 and 0.086 chord aft of the true apex, the calculations being based on eight rows of five points and five rows of eight points respectively. The foremost pressure transducer was situated on the centreline chord at 0.075 chord, therefore the position of the transducer falls within the planform of the former (0.05) case but excluded from the latter (0.086) case.

7. Discussion of Results

7.1. Experimental Results

No general statistical assessment of scatter was made. Although in the main it appeared to fall within the range ± 10 per cent, there were a number of 'rogue' readings. Some possible causes for their occurrence are discussed below.

Scatter was to some extent due to the tests being made over a range of amplitudes.

The R.A.E. 5 ft Tunnel has been shown⁷ to suffer from a high level of turbulence, and is therefore not well suited for making low-speed oscillatory pressure measurements.

At some points on the model the phase angle between pressure and motion was observed to drift over long periods, thus causing some of the readings to be indeterminate. No cause of drift could be established.

Because of the extremely low pressure differentials between upper and lower surfaces the signal output of individual transducers was very small. A high degree of amplification was therefore necessary, and so any errors introduced, either by the system of calibration, or by the method of recording, tended to be accentuated.

The reading and recording system adopted was very slow in operation and so tunnel runs were necessarily long. Thus the ambient conditions could change during the run, and drifts in sensitivity of the whole recording system could have occurred undetected in between the routine calibrations.

It was not easy to allow for the wear that took place in the swash-plate excitation system. An attempt was made to alleviate the problem by tuning the whole system to 5 Hz but some back-lash effects remained. The method of using strain gauges to check the model deformation was not as sensitive as could have been wished, and would not have detected changes smaller than 5 per cent. In addition, it could not take account of any possible variation in the plastic foam profile due to air loads, or variations of the foam properties⁸ due to environmental changes. In consequence changes in mode shape might have occurred.

The pressure transducers proved reliable and consistent; measurements of pressure taken under quasi-static conditions (1/300 Hz) indicated that the rate of the drift was very small. The calibration procedure was, however, laborious and time-consuming—a minimum of 30 minutes being required for each calibration sequence.

7.2. Calculated Values of Pressure

Difficulties have been experienced with collocation methods when calculating overall forces. The standard method does not calculate the downwash very accurately near the edges of the wing. It has been suggested^{9,10}, that by increasing the number of the spanwise integration points, accuracy may be improved, particularly when making calculations on wings of high aspect ratio. There remains, however, the difficulty which arises because of the sharp apex angle of a delta planform. Since the above suggested method shows no advantage on this score, and since it has only been programmed for the limiting case when the frequency tends to zero, the standard method was adopted in this experiment. Woodcock¹¹ has indicated that in the aspect ratio range 1 to 2, calculations of overall forces may be made to fair accuracy if they are based on at least 36 collocation points arranged in six rows of six. Because of the low aspect ratio (span/mean chord = 1.05) of this wing the best compromise within the programme limitation was considered to be an arrangement of collocation points having eight rows with five points in each row. Justification for this preference is contained in the calculated pressure distributions (Figs. 9 to 15) and comparison with measured values.

From Figs. 9 to 15 it can be seen that whilst the arrangement of collocation points is not critical (in practical terms) over the broad area of the wing, disposition can result in large alterations in the predicted values of pressure near the apex of a slender delta wing; the present programme does not seem to be very satisfactory for making accurate predictions in this region.

7.3. Comparison of Theory with Experiment

Fig. 9 shows the in-phase components of pressure distributed along the centreline chord of the model as calculated using both arrangements of collocation points; it also shows the measured values. Calculations based on five rows of eight points result in a distribution in which negative pressures near the (artificial) leading edge change in a short distance to positive pressures. The maximum value occurs fairly well forward and the pressure then drops steadily to the trailing edge. The other arrangement of collocation points allows the planform in the region of the apex to be represented more closely; by comparison with the first arrangement the positive hump in the pressure distribution has a maximum value that is higher and further aft, and the gradient ahead of the hump is less steep. If the actual

platform could have been represented accurately in the calculations it appears that the characteristics observed experimentally would be confirmed. In this case, the hump would have been still further aft, and the gradient ahead of the hump even less steep.

The in-quadrature components (Fig. 10) are much smaller and show less discrepancy between theory and experiment.

In the region of the apex, discrepancies between theory and experiment may be put down to the foreshortening of the nose that the theoretical technique implies. However, in an actual aircraft, pressures in this region are normally affected by the presence of a fuselage.

Over the main body of the wing there is good agreement between theory and experiment of both the in-phase and the in-quadrature pressure components within the range of frequency parameters employed.

In considering the above comparisons and deductions, it should be borne in mind that the method of calculation was originally devised to give the generalised forces, with the collocation points derived as best for this purpose. The programme, as modified to give pressure distribution, relied upon the same derivation of collocation points, whereas, the best collocation data for determining pressure at a point may well differ.

8. Concluding Remarks

The purpose of these experiments was to compare values of oscillatory pressures calculated using a computer programme of D. E. Davies with those measured experimentally in a low-speed wind tunnel on a slender delta model vibrating in a bending mode. It was found that over the main area of the wing there is good agreement between theory and experiment of both in-phase and in-quadrature components at a series of amplitudes with frequency parameters ranging from 0.5 to 0.8.

The notable discrepancies can be ascribed to the inability of the theory to cater for the very acute apex angle of the slender delta shape; these discrepancies occur mainly in an area normally occupied by the fuselage of an aircraft and so any calculations of oscillatory pressures in these regions are therefore subject to other, possibly much larger, uncertainties.

The experimental scatter was rather greater than desirable; together with other causes, difficulties in developing a satisfactory technique for day-to-day calibrations of the pressure transducers were suspected, rather than any shortcomings in the transducers themselves. In general the transducers proved to be suitable for this type of measurement, and the construction could well be modified to suit other similar requirements.

Acknowledgements

Acknowledgements are due to Dr. W. G. Molyneux for the original planning and advice given throughout the experiments; and also to Mr. W. G. Jenkins and Staff of the R.A.E. Inspection Department for the precise determination of the positions of pressure points on the model and provision of the applicable ordinates table.

REFERENCES

- | <i>No.</i> | <i>Author(s)</i> | <i>Title, etc.</i> |
|------------|---|--|
| 1 | W. R. Laidlaw | Theoretical and experimental pressure distribution on oscillating low aspect ratio wings.
M.I.T. T.R. 51-52 (1954). |
| 2 | H. Bergh | A new method for measuring the pressure distribution on harmonically oscillating wings.
M.L.R. Report MT224 (1964). |
| 3 | W. G. Molyneux and
F. Ruddlesden | A technique for the measurement of pressure distribution on oscillating aerofoils with results for a rectangular wing of aspect ratio 3.3.
A.R.C. C.P. 233 (1955). |
| 4 | H. C. Lessing, J. L. Troutman
and G. P. Menees | Experimental determination of the pressure distribution on a rectangular wing oscillating in the first bending mode for Mach numbers from 0.24 to 1.30.
NASA TN D-344 (1960). |
| 5 | S. A. Leadbetter,
S. A. Clevenson and W. B. Igoe | Experimental investigation of oscillating aerodynamic forces, moments and pressures acting on a tapered wing oscillating in pitch at Mach numbers from 0.40 to 1.07.
NASA TN D-1236 (1962). |
| 6 | D. E. Davies | Calculation of unsteady generalised air forces on a thin wing oscillating harmonically in subsonic flow.
A.R.C. R. & M. 3409 (1963). |
| 7 | C. A. K. Irwin and
P. R. Guyett | The subcritical response and flutter of a swept-wing model.
A.R.C. R. & M. 3497 (1965). |
| 8 | D. B. Payen | Stiffness, damping and creep properties of a polyurethane foam including the effects of temperature and humidity.
A.R.C. C.P. 905 (1963). |
| 9 | H. C. Garner | Accuracy of downwash evaluation by Multhopp's lifting-surface theory.
A.R.C. R. & M. 3431 (1964). |
| 10 | H. C. Garner | ALGOL 60 programme for Multhopp's low-frequency subsonic lifting-surface theory.
A.R.C. R. & M. 3517 (1966). |
| 11 | D. L. Woodcock | On the accuracy of collocation solutions of the integral equation of linearised subsonic flow past an oscillating aerofoil.
<i>Proceedings of the International Symposium on Analogue and Digital Techniques Applied to Aeronautics, Liege 9-12 September 1963.</i> |

APPENDIX A

Measurement of Mode Shape

A.1. Equipment used

A Wayne-Kerr Vibration Meter was used to measure the vertical oscillatory displacement of points distributed over the upper surface of the wing. A moveable measuring head, itself supported on a surface erected beneath the wing, was connected to each point in turn. The apparatus is shown in Fig. 7.

A.2. Measuring Head

The measuring head consisted of a heavy base having a vertical column, the top of which supported a cantilever beam. The measuring probe was fixed to the extremity of the beam. A hinged parallel-link system was secured to the vertical column so that a horizontal plate attached to the top of the parallel-link system registered with the measuring probe; a second similar probe and plate mounted inboard was used for check measurements. The distance separating the probe and plate was indicated on the vibration meter. Coupling between the parallel link and the wing was by a stiff wire. Each end of the wire had a ball and socket adaptor, one secured to the moveable end of the link system, and the other attached to any desired point on the surface of the wing by temporary adhesive. Springs within the parallel link system enabled it to be tuned to the wing excitation frequency (5 Hz), thus ensuring that the surface of the wing was loaded only by the damping forces in the link system which were negligibly small.

A.3. Monitoring Points

A probe and complementary disc were positioned beneath the under surface of the wing midway between the forcing trunnions, and a similar set was positioned to measure the throw of the swash-plate connecting rod. Checks at these points ensured constant amplitude at the forcing points during the mode measurement.

A.4. Method of Measuring Mode Shape

A close grid was marked on the upper surface of the wing. The measuring head was positioned so that the upper ball and socket adaptor was directly above an intersection of the grid ordinates. The lower ball and socket adaptor was then secured to the wing with temporary adhesive at the point of intersection. When the wing was vibrated at 5 Hz, the vertical displacement of the chosen point was indicated on the vibration meter. Similar measurements were made at each intersection of the ordinates in turn, and the procedure was repeated to give mode shape data for each of the three set amplitudes of vibration.

No flexing across the span of the model was detected during the mode measurements.

APPENDIX B

Determination of Pressure Transducer Characteristics

B.1. Pre-installation Tests

Since the basic components of the transducers used for the slender-wing experiments were derived from the transducers described in Ref. 3, it was expected that the dynamic characteristics of each type would be similar. However, proof checks were made. Acoustic excitation indicated that the resonance frequency of the diaphragms was in the region 200 Hz; and when the transducer was subjected to oscillatory motion parallel to the transducer centreline, no adverse inertia effect was evident when the frequency was 20 Hz and the amplitude was ± 1.5 in (± 38 mm).

B.1.1. Post-installation and serviceability checks. After installing the model and recording equipment in the wind tunnel, proof checks were made to establish overall serviceability, and that the strains created when the model was vibrated did not manifest themselves as spurious outputs from the pressure transducers. The checks consisted of testing each transducer for possible air leaks within the working

pressure range, static calibrations, and checking the transducer outputs when the model was vibrated in still air.

B.2. Primary Static Calibration

The characteristics of the pressure transducers when subjected to static pressures within a range of 0 to 20 lbf/ft² (960 N/m²) were obtained using the equipment shown in Fig. 16. Except for the pressure transducer fitted in the nose of the model all the transducers were enclosed by the inverted box clamped to the wing. Thus one side of the enclosed transducers was subjected to the pressure existing within the box, the opposite side being exposed to atmospheric pressure. The box was pressurised from a (suitably reduced) compressed air supply and the internal pressure was adjusted as required by a leak-valve. Tappings enabled the pressure to be measured by a precision manometer, and connections to be made to extraneous pressure transducers *viz* at the model nose position and the test sets (described later). By this means all the pressure transducers were calibrated in a common environment. The output signal from each transducer was found to be linear when:

- (a) the applied voltage was constant and the pressure varied,
- (b) when the applied pressure was constant and the voltage varied.

B.3. Dynamic Calibrations

Routine calibrations of the pressure transducers were made dynamically. A fluctuating pressure within the range of $\pm 5\frac{1}{2}$ lbf/ft² (± 260 N/m²) was generated by a pump that could be coupled to the driving rod of the swash-plate unit. The wing drive was disconnected during the transducer calibration operations.

B.3.1. Pump characteristics. The calibrating pump consisted of a thick-walled cylindrical chamber having a plunger set in the centre of one face. The bearing of the plunger was sealed by means of a stiff bellows-type gland. The opposite face was tapped to allow the internal pressure to be sensed externally. To operate the pump one end of a centre-pivoted lever was connected to the pump plunger, and the opposite end could be coupled to the horizontal driving rod of the swash-plate unit, thereby providing motion of variable amplitude and frequency. The arrangement of the pump and drive is shown diagrammatically in Fig. 17. The relationship between the plunger stroke and the (static) pressure developed was established by calibrating the stroke against the pressure indicated on a precision pressure gauge that was connected to the pump. Concurrently the output from a pressure transducer also connected to the pump was recorded. The relationship of the pressure and transducer output with the pump plunger stroke proved to be linear, and when the swash-plate was operated at 5 Hz the displayed signal from the transducer was sinusoidal. Transition from isothermal to adiabatic conditions within the pump were found to be virtually complete at frequencies above 0.5 Hz. Fig. 18 shows the pressure/frequency curve obtained when the pump was run at constant stroke and the frequency was varied from a quasi-static condition (1/300 Hz) to 10 Hz. It will also be seen that the static-dynamic pressure ratio at the normal operating frequency (5 Hz) is 1:1.4.

Because the transducers in the wing were situated some distance from the pump a connecting pipe of about 5 ft (1.5 m) length was required; consequently the effect due to pipe length had to be determined. This was done by comparing the output from a transducer adjacent to the pump with one connected to the pump by a length of tubing. The pump was run at a set stroke and frequency and the output from each transducer measured. The operation was repeated with tubing of different lengths, the maximum length tested being 35 ft (10.7 m). The nominal bore size of all the tubes was 0.25 in (6.35 mm) diameter. The resulting curve is given in Fig. 19, and it can be seen that at the required length of 5 ft (1.5 m) only negligible effect on the pressure prevails.

B.3.2. Peripheral equipment. Dynamic calibration depended upon measuring the dynamic pressure generated by the pump and monitoring the pressure at the end of the connecting tubing used to pressurise the transducer in the wing. This was done by using two similar independent test sets. Each test set was self-contained and comprised a pressure transducer set in foam (as fitted in the wing) plus energising battery, voltmeter and adjustable resistance for indicating and setting the transducer sensitivity. One of the test sets was situated at, and connected to, the pump. A standard sensitive pressure

gauge was also connected to the pump. The second test set was connected to the pump by a 5 ft (1.5 m) length of 0.25 in (6.35 mm) bore flexible tubing, thus allowing the test set to rest upon the upper surface of the wing. A spring-loaded spigot-type connector, coupled to the second test set by a T-joint, enabled pressure to be fed into any transducer fitted to the wing. The test set equipment is shown in situ for testing in Fig. 20.

B.4. *Method and Sequence of Routine Calibration*

The following calibrating routine was carried out immediately prior to, and at the completion of, each sequence of measurement of the unsteady pressures over the wing.

With the pump test sets connected as described above, a combined leak check, summary static and dynamic calibration was carried out as follows:

- (a) Blank off outlet at the wing transducer connection.
- (b) Set stroke of pump to $\frac{1}{3}$ of maximum stroke.
- (c) Rotate swash-plate by hand, pausing at the maximum and minimum throw positions to allow self-generated heat to dissipate within the system. Note respective pressures indicated on the sensitive pressure gauge and derive the relationship pump stroke/pressure developed.
- (d) Run pump at 5 Hz and note output voltage of each test set.
- (e) Repeat sequence (c) and (d) with pump stroke set to $\frac{1}{2}$ maximum throw, followed by further repeat at maximum pump throw.

From relationships, pump stroke against static pressure generated by the pump, and the pump stroke against transducer output at a pump frequency of 5 Hz, a dynamic calibration of transducer output volts against apparent pressure can be made. By applying the specific heat ratio factor for air (1.4), the dynamic calibration expression becomes transducer output volts against real (adiabatic) pressure pertaining within the pump at 5 Hz. By this means, dynamic calibration curves were obtained for each test set. The calibration curves proved to be linear. Each transducer in the wing was then dynamically calibrated by removing the blank from the connecting tube and connecting the pressure line to the transducer under test. The pump was operated at 5 Hz, and the outputs from each test set were cross-related with the wing transducer output to obtain the required dynamic calibration of output volts against pressure.

B.5. *General Characteristics*

Throughout the experiment the pressure transducer proved to be reliable and consistent. Measurements taken under quasi-static conditions (1/300 Hz) indicated that the rate of drift was very small. Pressure distribution measurements, made under near-static conditions (1/7 Hz), proved that the transducers were well capable of this type of measurement.

The above qualities were, in part, due to the transducers possessing the required sensitivity although the applied voltage at the transducer strain-gauge bridge was only half the safe working voltage. In general, the manufacture of the transducer is straightforward, although a fair degree of skill is required when applying the windings.

TABLE 1

Measured Non-Dimensional Pressures—Frequency Parameter = 0.507

Pressure point ordinate		Pressure components —amplitude = Z_{xp}				Pressure components —amplitude = $2Z_{xp}$				Pressure components —amplitude = $3Z_{xp}$			
X	Y	First measurements		Repeat measurements		First measurements		Repeat measurements		First measurements		Repeat measurements	
		In-phase	In-quadrature	In-phase	In-quadrature	In-phase	In-quadrature	In-phase	In-quadrature	In-phase	In-quadrature	In-phase	In-quadrature
0.0815	0.0006	-2.9899	0	-3.3370	0	—	—	-2.7910	-0.0240	-1.7780	0	-2.5990	0
0.1575	0.0224	-1.9230	-0.2020	—	—	-1.6380	-0.1430	-1.9020	-0.2170	-1.8420	-0.2590	-1.8570	-0.1790
0.2458	0.0162	-0.2470	-0.5070	—	—	-0.4360	-0.5190	-0.3910	-0.6020	—	—	-0.3950	-0.4700
0.2463	0.0503	-0.9150	-0.4070	-0.5920	-0.3550	-0.7650	-0.3400	-0.9810	-0.3960	-0.8450	-0.3940	-0.8460	-0.4120
0.3478	0.0001	+1.4942	-0.5440	+1.6060	-0.5850	+1.4880	-0.5410	+1.4610	-0.5610	+1.4250	-0.5460	+1.3460	-0.6280
0.3478	0.0369	0.6840	-1.4670	1.4560	-0.9100	1.1630	-0.4980	1.2040	-0.4860	1.2790	-0.4660	1.1890	-0.5300
0.3479	0.0756	0.4470	-0.5330	0.4710	-0.4880	0.4410	-0.5850	0.4320	-0.5740	0.3690	-0.4900	0.3128	-0.4820
0.4746	0.0010	3.3980	-0.1780	3.6200	-0.2530	2.9800	-0.2080	3.0610	-0.1600	3.1120	-0.1090	2.8170	-0.3460
0.4749	0.0373	2.7730	-0.3410	3.6720	-0.6470	—	—	2.6240	-0.4160	3.0640	-0.3220	2.8800	-0.4050
0.4749	0.0752	2.5630	-0.3150	2.6220	-0.2750	2.1910	-0.2700	2.3350	-0.2870	2.3330	-0.2450	1.8250	-0.2560
0.4745	0.1176	1.5240	-0.3240	1.6420	-0.3490	1.7070	-0.3630	1.5490	-0.3130	1.3330	-0.3200	1.3680	-0.3920
0.6307	0.0012	3.7160	0	3.7690	0	—	—	4.2300	0	3.4640	+0.1210	3.3880	—
0.6271	0.0652	3.2030	0	—	—	3.1690	0	3.243	0	3.4720	0	3.1600	0.2210
0.6284	0.1087	3.3050	0	3.2460	+0.1700	3.1290	0	3.010	0	3.2000	0	3.0540	0
0.6274	0.1527	3.2600	0	3.2830	0.0600	3.0940	0	3.1350	0	2.9740	0	3.3524	-0.1170
0.7797	0.0005	2.4730	0.5710	2.7140	0.6270	2.7160	+0.7790	2.4960	+0.7160	2.7300	0.5800	2.5940	0.4570
0.7794	0.0429	2.4430	+0.5190	2.4630	0.5690	2.5050	0.4870	2.5300	0.5380	2.6600	0.5410	2.4600	0.3900
0.7796	0.0861	2.7880	0.4940	2.7530	0.5350	2.5250	0.4450	2.5740	0.5470	2.939	0.5710	2.772	0.3400
0.7802	0.1289	2.9590	0.3630	3.0580	0.3750	2.9300	0.3600	3.0550	0.4270	2.9710	0.4700	3.0280	0.2650
0.7798	0.1725	3.2970	0.2880	3.7100	0.3900	3.2920	0.1730	3.4960	0.2140	3.2370	0.3400	3.3100	0.1160
0.9448	0.0531	1.1070	0.6650	1.2300	0.6820	1.1160	0.6470	1.1240	0.6490	1.3140	0.6700	0.8910	0.4160
0.9448	0.1601	1.3490	0.6290	1.3350	0.6220	1.2720	0.5400	1.4760	0.5970	1.5170	0.6130	1.4270	0.5200
0.5501	0.1469	1.679	-0.1170	1.6540	-0.1450	1.1220	0	1.3940	0	2.1560	-0.2660	—	—
0.6256	0.1788	3.328	-0.1160	3.4730	-0.3040	3.2580	-0.2280	3.5240	-0.2460	3.1900	-0.2510	3.3000	-0.4640

X = Distance of point aft of apex (metre).

Y = Distance of point from centreline (metre).

 $Z_{xp} = 3.48 \text{ mm} = \frac{1}{2} \times \text{total displacement at the point of excitation.}$

TABLE 2
Measured Non-Dimensional Pressures—Frequency Parameter = 0.616

Pressure point ordinate		Pressure components —amplitude = Z_{xp}				Pressure components —amplitude = $2Z_{xp}$				Pressure components —amplitude = $3Z_{xp}$			
X	Y	First measurements		Repeat measurements		First measurements		Repeat measurements		First measurements		Repeat measurements	
		In-phase	In-quadrature	In-phase	In-quadrature	In-phase	In-quadrature	In-phase	In-quadrature	In-phase	In-quadrature	In-phase	In-quadrature
0.0815	0.0006	-2.9870	-0.4200	-3.0130	0	-2.8720	0	-2.9060	0	-2.6450	0	-2.7570	-0.0962
0.1575	0.0224	-2.0650	-0.4390	-2.0920	-0.2940	-1.8220	-0.2240	-1.8380	-0.2580	—	—	-1.3750	-0.2420
0.2458	0.0162	-0.2450	-0.8530	-0.3070	-0.8440	-0.3370	-0.7230	-0.2050	-0.7130	-0.3190	-0.5530	-0.2130	-0.5260
0.2463	0.0503	-0.7180	-0.4660	-0.9140	-0.5270	-0.6850	-0.3800	-0.7780	-0.6080	-0.7780	-0.4670	-0.7770	-0.5050
0.3478	0.0001	+1.7540	-0.5700	+1.6430	-0.8820	+1.6690	-0.7080	+1.7040	-0.6890	+1.6100	-0.6830	+1.6120	-0.6190
0.3478	0.0369	0.9170	-0.3160	1.5180	-0.6780	0.9600	-0.5540	0.7230	-0.3530	1.1860	-0.5780	1.3850	-0.5880
0.3479	0.0756	0.5200	-0.5780	0.4630	-0.7410	0.4640	-0.6390	0.4900	-0.7260	0.4700	-0.5800	0.3430	-0.4720
0.4746	0.0010	3.7030	-0.1290	3.3210	-0.2320	3.3220	-0.2910	3.0780	-0.2150	3.0790	-0.2150	2.5180	-0.1760
0.4749	0.0373	3.2710	-0.4020	3.1800	-0.6180	3.1100	-0.5490	3.1780	-0.5600	2.9110	-0.4610	2.3240	-0.4800
0.4749	0.0752	2.7870	-0.3420	2.7950	-0.4430	2.6540	-0.3730	2.7330	-0.5310	2.6490	-0.3720	2.2060	-0.2710
0.4745	0.1176	1.5860	-0.4250	1.6410	-0.4710	1.6070	-0.4300	—	—	1.6740	-0.4170	1.5520	-0.3870
0.6307	0.0012	3.7900	0	4.0380	0	3.8720	+0.2030	—	—	3.9360	+0.1720	3.3850	+0.1770
0.6271	0.0652	3.2870	0.1150	3.5890	0	3.3330	0.0580	3.5320	0	3.4080	0.1190	3.802	0.1330
0.6284	0.1087	3.2370	0.2840	3.5880	0	3.4130	0.2390	3.3400	+0.0580	3.4770	0.1150	3.3360	0.1750
0.6274	0.1527	3.2720	0	3.4860	0	3.6460	0	3.6470	0.0640	3.1430	0	3.1960	0
0.7797	0.0005	2.8520	0.9270	2.9660	0.8510	3.4580	0.9490	2.4000	0.6870	2.6180	0.7750	2.4780	0.7580
0.7794	0.0429	2.500	0.6700	2.5650	0.7350	2.3130	0.5770	2.4880	0.7130	2.4770	0.7100	2.1730	0.6230
0.7796	0.0861	2.7420	0.7350	2.9510	0.7360	2.1970	1.3730	—	—	2.7840	0.6940	2.4620	0.6050
0.7802	0.1289	2.9210	0.5680	3.2200	0.4480	3.0570	0.5390	3.0160	0.4780	3.0430	0.5640	3.1020	0.5470
0.7798	0.1725	3.4500	0.4850	3.8830	0.4220	3.6610	0.3200	3.8510	0.4050	3.5730	0.3760	3.6970	0.4210
0.9948	0.0531	1.0370	0.8400	1.2620	0.8830	1.1830	0.8600	1.5310	1.0720	1.1390	0.798	0.8870	0.6210
0.9448	0.1601	1.2630	0.7000	1.4420	0.7750	1.5100	0.7370	1.5050	0.7340	1.4880	0.758	1.0680	0.5440
0.5501	0.1469	1.0290	-0.4160	3.3840	-0.4200	1.2300	-0.0430	—	—	—	—	—	—
0.6256	0.1788	3.5280	-0.3090	3.8930	-0.3410	3.7050	-0.3240	—	—	3.4800	-0.305	3.4990	-0.3060

14

X = Distance of point aft of apex (metre).

Y = Distance of point from centreline (metre).

$Z_{xp} = 3.48 \text{ mm} = \frac{1}{2} \times \text{total displacement at the point of excitation.}$

TABLE 3

Measured Non-Dimensional Pressures—Frequency Parameter = 0.797

Pressure point ordinate		Pressure components —amplitude = Z_{xp}				Pressure components —amplitude = $2Z_{xp}$				Pressure components —amplitude = $3Z_{xp}$			
X	Y	First measurements		Repeat measurements		First measurements		Repeat measurements		First measurements		Repeat measurements	
		In-phase	In-quadrature	In-phase	In-quadrature	In-phase	In-quadrature	In-phase	In-quadrature	In-phase	In-quadrature	In-phase	In-quadrature
0.0815	0.0006	-3.0753	-0.2150	-2.8010	-0.0980	-2.7810	-0.1490	-2.7810	-0.0480	-2.7820	-0.0970	-2.7000	-0.0940
0.1575	0.0224	-2.0450	-0.4720	-1.7480	-0.3720	-1.8210	-0.4200	-1.6630	-0.4140	-1.8440	-0.4540	-1.7430	-0.4340
0.2458	0.0172	-0.2028	-0.0300	-0.3000	-1.0480	-0.2720	-0.8910	-0.2420	-0.8450	-0.2400	-0.8360	-0.258	-0.7930
0.2463	0.0503	-0.9745	-0.6510	-0.7640	-0.5970	-0.7610	-0.6394	-0.7540	-0.6330	-0.7960	-0.6920	-0.779	-0.6310
0.3478	0.0001	+2.0690	-0.7120	+2.0280	-0.6600	+2.0210	-0.7760	+1.5840	-1.5310	+1.9240	-0.7450	+1.8860	-0.7240
0.3478	0.0369	1.4650	-0.5620	1.2090	-0.3770	0.4870	-0.3700	0.5670	-0.6300	1.526	-0.7780	0.6710	-0.6260
0.3479	0.0756	0.7510	-1.0720	0.7040	-0.9690	0.8130	-1.3020	—	—	0.4540	-0.7560	0.4400	-0.7320
0.4746	0.0010	3.5392	-0.0620	3.7480	-0.1950	3.3520	0	3.2920	0	3.4020	-0.2980	3.0740	-0.2690
0.4749	0.0373	3.7867	-0.6680	3.1960	-0.5640	3.5310	-0.8140	3.5500	-0.7540	3.5350	-0.8810	3.2500	-0.4570
0.4749	0.0752	3.0290	-0.5340	2.8240	-0.5490	2.8270	-0.6520	2.8200	-0.4980	2.8570	-0.4010	2.7220	-0.3340
0.4745	0.1176	1.8590	-0.6760	1.7450	+0.4680	—	—	—	—	1.5950	-0.5180	1.5440	-0.4720
0.6307	0.0012	4.4290	+0.1550	4.0640	0.2130	4.9950	0.1740	4.9890	0.1740	4.0690	+0.3200	3.9000	+0.3070
0.6271	0.0652	3.5240	0	3.3080	0	3.4180	0	3.3810	0	3.5260	0.2160	3.3960	0.2370
0.6284	0.1087	3.7440	0.1960	3.4170	0	3.4280	0	3.4700	0.0600	3.9870	0.2790	3.402	0.2370
0.6274	0.1527	3.7880	0.1980	3.4270	0	3.4980	0	3.6190	0	3.4580	0	3.3920	0
0.7797	0.0005	3.8990	0.9420	2.8970	1.0540	2.8120	0.968	2.8720	1.0460	2.6800	0.9760	2.6110	0.9760
0.7794	0.0429	2.5520	0.9290	2.4150	0.8790	3.4570	1.258	3.3420	1.1510	2.5710	0.9360	2.5510	0.9280
0.7796	0.0861	2.9530	1.0170	2.7660	0.8990	2.8350	0.894	2.6910	0.9800	2.820	0.9160	2.6880	0.8730
0.7802	0.1289	3.1700	0.8500	3.0080	0.6390	3.0690	0.652	3.0890	0.6010	3.0870	0.7700	2.9440	0.7340
0.7798	0.1725	3.8320	0.6070	3.6900	0.4530	4.0290	0.4950	3.9910	0.4200	3.7890	0.5660	3.6730	0.5820
0.9448	0.0531	1.4060	1.2660	1.3720	1.1510	1.4430	1.1280	1.4460	1.2130	1.2600	1.0580	1.1940	1.0340
0.9448	0.1601	1.6040	1.1230	1.3070	1.0960	1.3550	0.9850	1.5620	1.2200	1.4860	1.0000	1.4570	0.9460
0.5501	0.1469	1.3700	-0.4330	1.7030	-0.4470	2.7870	-0.6440	2.6750	-0.9240	2.608	-0.5540	2.2670	-0.4800
0.6256	0.1788	4.0580	-0.4260	3.6490	-0.4480	3.6980	-0.4540	3.7140	-0.2600	3.2620	-0.2850	3.4260	-0.6660

X = Distance of point aft of apex (metre).

Y = Distance of point from centreline (metre).

 $Z_{xp} = 3.48 \text{ mm} = \frac{1}{2} \times \text{total displacement at the point of excitation.}$

TABLE 4

Calculated Non-Dimensional Pressures at Pressure Points of Model

Pressure transducer co-ordinates		Collocation data : 5 chordwise sections in semi-span \times 8 points						Collocation data : 8 chordwise sections in semi-span \times 5 points					
X	Y	$v = 0.5069$		$v = 0.616$		$v = 0.797$		$v = 0.5069$		$v = 0.616$		$v = 0.797$	
		In-phase	In-quadrature	In-phase	In-quadrature	In-phase	In-quadrature	In-phase	In-quadrature	In-phase	In-quadrature	In-phase	In-quadrature
		← Off model planform →											
0.0815	0.0006							-5.09961	-0.26207	-5.10081	-0.31896	-5.11156	-0.41309
0.1575	0.0224	-2.29307	-0.45878	-2.31036	-0.55659	-2.33893	-0.72222	-2.69755	-0.72876	-2.69116	-0.88517	-2.69314	-1.14877
0.2458	0.0162	+1.68501	-0.59807	+1.68321	-0.72435	+1.68963	-0.93658	+0.08928	-0.74870	+0.10770	-0.90517	+0.13730	-1.16632
0.2463	0.0503	-0.25541	-0.64586	-0.25029	-0.78103	-0.23136	-1.00531	-0.86096	-0.75130	-0.84378	-0.90870	-0.81958	-1.17187
0.3478	0.0001	+2.96166	-0.60769	+2.98370	-0.73373	+3.02857	-0.94473	+2.57746	-0.58162	+2.60421	-0.69985	+2.66201	-0.89602
0.3478	0.0369	+2.79209	-0.57226	+2.80926	-0.69077	+2.84767	-0.88850	2.26578	-0.57597	2.28971	-0.69325	2.34044	-0.88780
0.3479	0.0756	+1.12751	-0.50452	1.13990	-0.60986	1.17185	-0.73373	1.38622	-0.64153	1.40644	-0.77339	1.44555	-0.99329
0.4746	0.0010	+3.85014	-0.28735	3.87689	-0.34402	3.93755	-0.43898	4.20563	-0.26137	4.22918	-0.31207	4.28957	-0.39654
0.4749	0.0373	3.73003	-0.29829	3.75424	-0.35717	3.80911	-0.45568	4.07087	-0.24497	4.09268	-0.29222	4.14931	-0.37071
0.4749	0.0752	3.50467	-0.30697	3.52295	-0.36725	3.56855	-0.46724	3.77411	-0.27116	3.79485	-0.32390	3.84781	-0.41137
0.4745	0.1176	1.62055	-0.22136	1.64028	-0.26780	1.68082	-0.34416	3.18599	-0.38888	3.20165	-0.46660	3.24141	-0.59632
0.6307	0.0012	3.98952	+0.31958	4.01231	+0.38534	4.07472	+0.50169	4.24010	+0.27714	4.25556	+0.33804	4.30206	+0.43938
0.6271	0.0652	3.88109	+0.26985	3.89759	0.32952	3.94441	0.42886	4.14419	0.26276	4.15952	0.32079	4.20592	0.41733
0.6284	0.1087	3.76581	+0.14316	3.77872	0.17767	3.81852	0.23524	3.99132	0.21284	4.00788	0.26059	4.05556	0.34024
0.6274	0.1527	3.33888	+0.15929	3.35412	0.19492	3.39351	0.25376	3.74058	0.13173	3.75314	0.16263	3.79114	0.21439
0.7797	0.0005	2.85027	0.78440	2.86687	0.94995	2.91131	1.22671	2.98357	0.79583	3.00020	0.96365	3.04541	1.24383
0.7794	0.0429	2.90533	0.75701	2.92057	0.91690	2.96336	1.18420	2.98312	0.77421	2.99819	0.93755	3.03987	1.21026
0.7796	0.0861	2.95054	0.70956	2.96313	0.85929	3.00099	1.10967	2.93151	0.73265	2.94522	0.88747	2.98398	1.14599
0.7802	0.1289	2.94496	0.61533	2.95780	0.74550	2.99350	0.96349	2.86547	0.64200	2.87728	0.77814	2.91148	1.00575
0.7798	0.1725	3.22575	0.42165	3.22947	0.51343	3.25273	0.66710	3.12384	0.49158	3.13094	0.59678	3.15598	0.77311
0.9448	0.0531	1.13785	0.75010	1.14507	0.90667	1.16230	1.16887	1.28737	0.91578	1.29819	1.10695	1.32362	1.42649
0.9448	0.1601	0.99570	0.71934	1.00058	0.87042	1.01222	1.12331	1.18341	0.77962	1.18939	0.94294	1.20499	1.21610
0.5501	0.1469	0.93145	-0.98217	0.94892	-1.18536	0.97113	-1.52269	2.104	-0.65990	2.11742	-0.79378	2.14689	-1.01651
0.6256	0.1788	4.15495	-0.35024	4.17200	-0.42377	4.19610	-0.54374	3.26696	-0.08434	3.27550	-0.09848	3.30250	-0.12157

X = Perpendicular distance from apex (metre).
 Y = Perpendicular distance from centreline (metre).

v = frequency parameter.

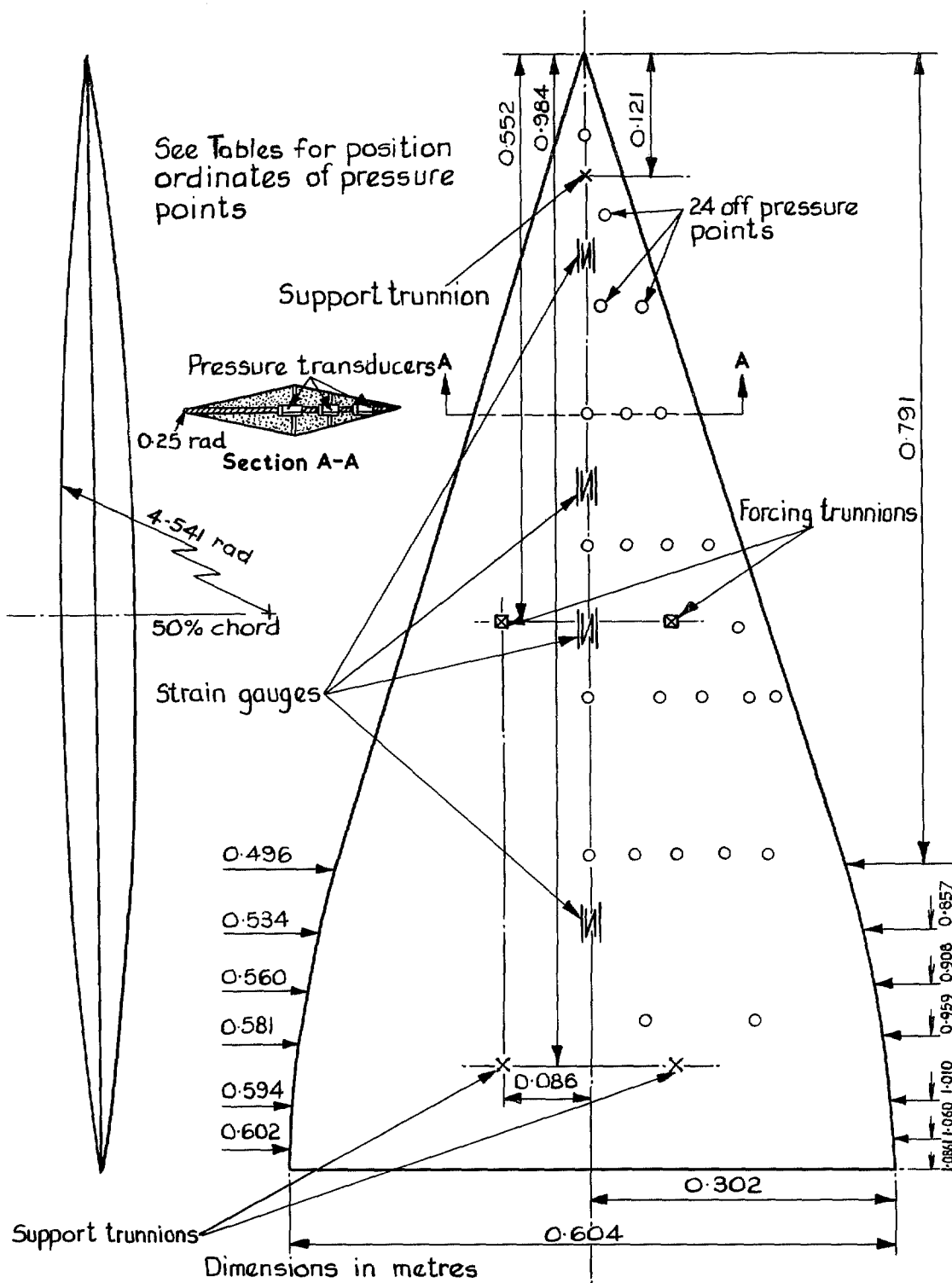


FIG. 1. Shape of model and disposition of transducers.

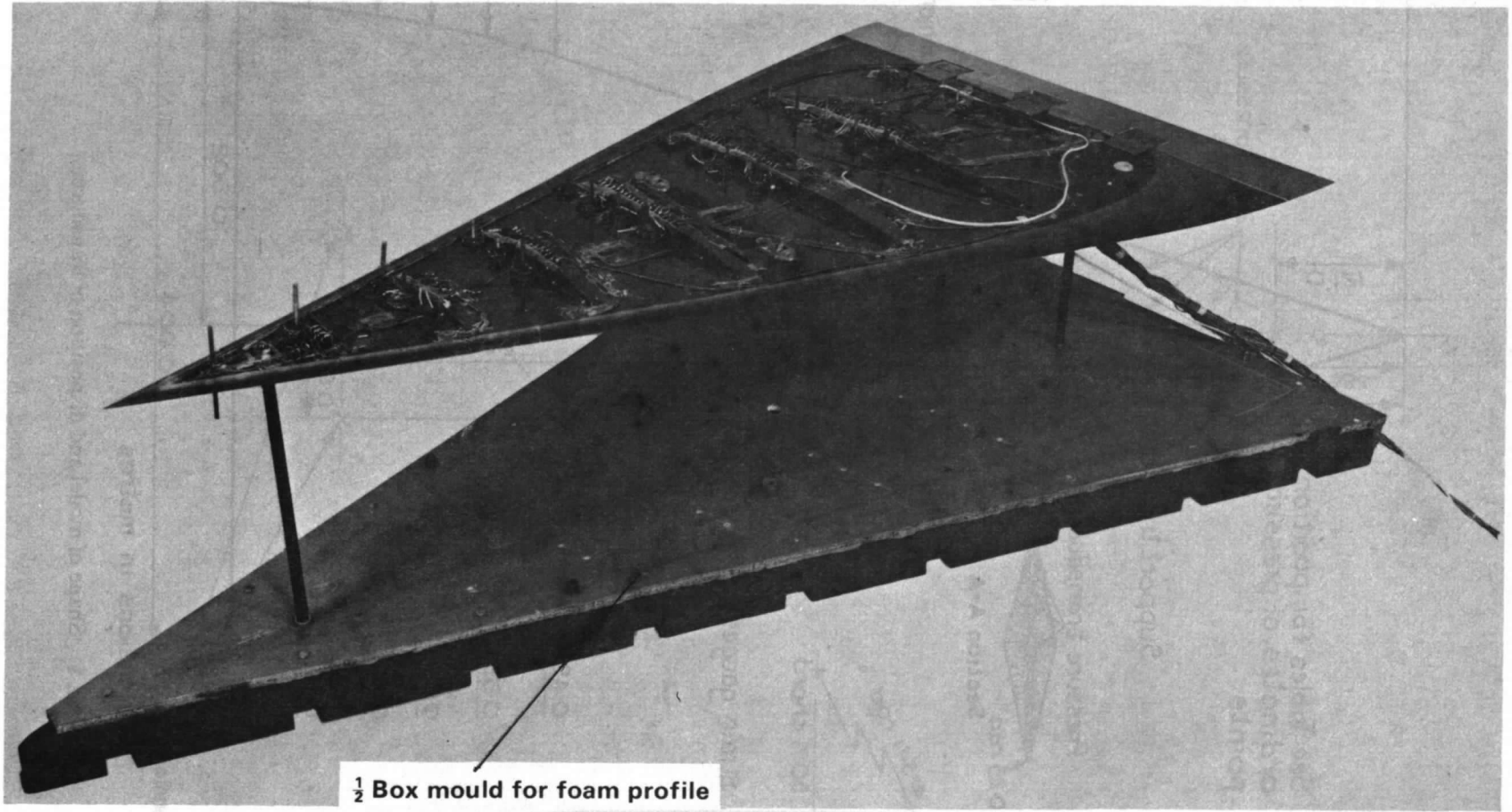


FIG. 2. Instrumentation of model—before application of foam.

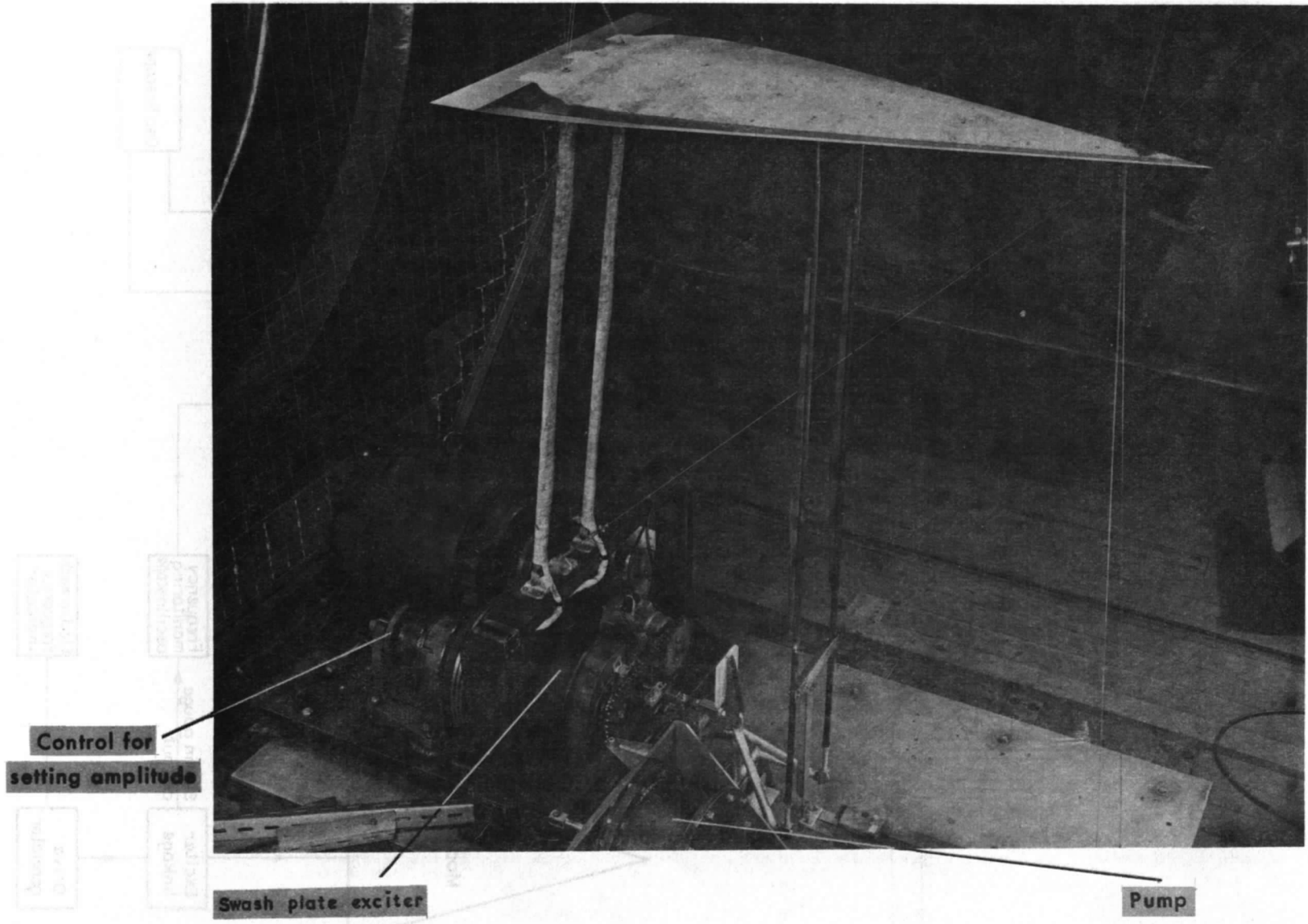


FIG. 3. Model support and excitation mechanism.

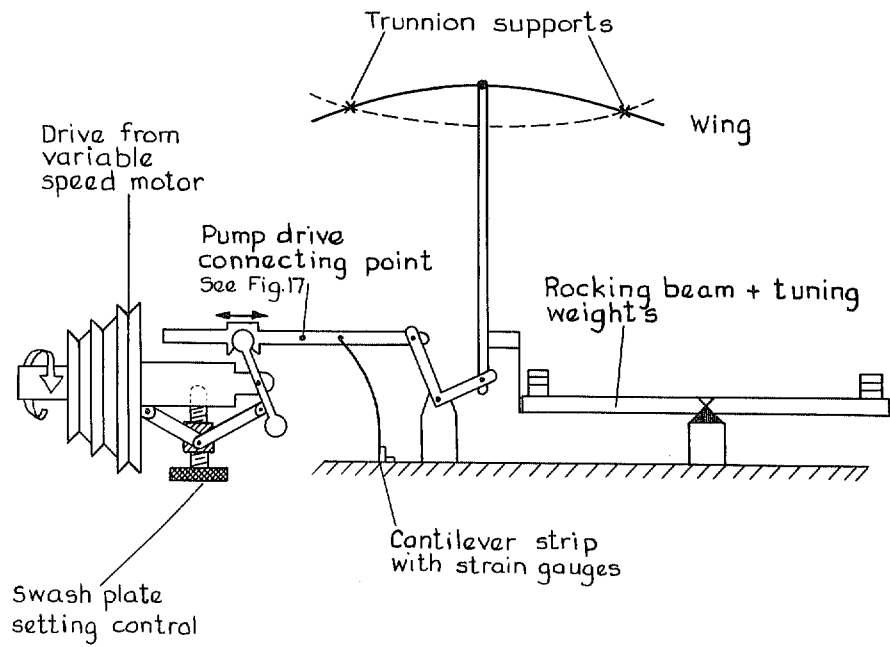


FIG. 4. Excitation system of model—diagrammatic.

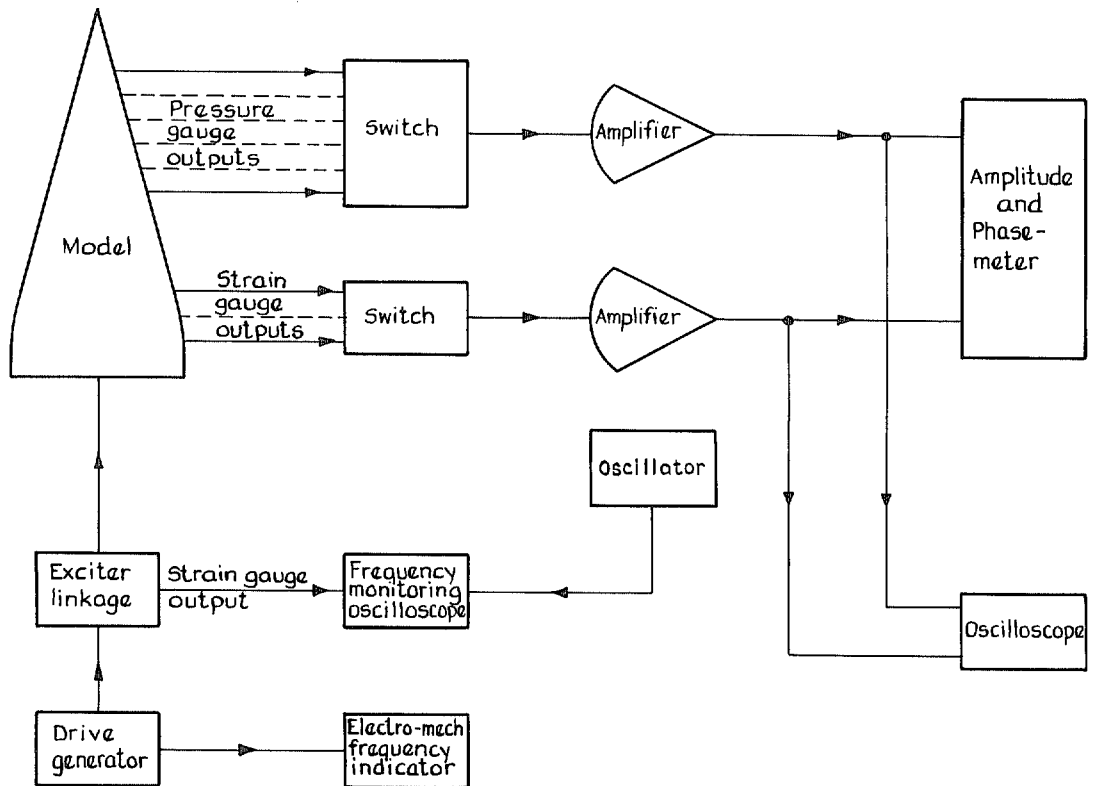
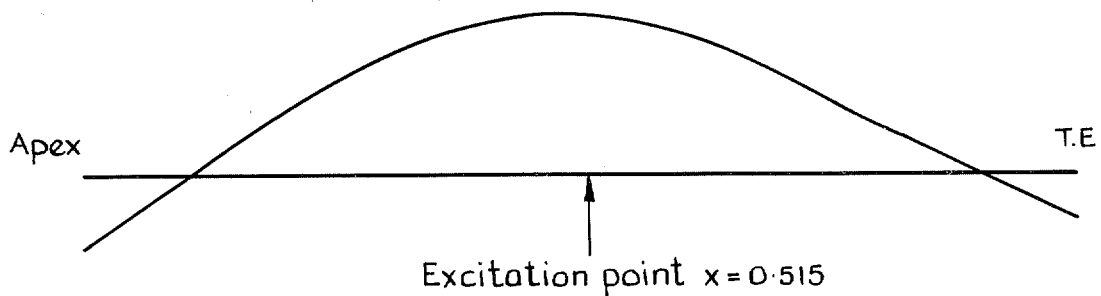


FIG. 5. Block diagram of the excitation and measuring procedure.



Deflected shape of the ζ chord
 (There was no flexing across the span)

x = Distance aft of the apex, as a fraction of ζ chord
 Y = Deflection, as a fraction of the maximum amplitude

x	0	0.1	0.2	0.3	0.4	0.45	0.48	0.5	0.55	0.6	0.7	0.8	0.9	1.0
Y	-0.46	-0.034	0.394	0.742	0.952	0.996	1.00	0.998	0.964	0.888	0.670	0.358	0.046	-0.282

FIG. 6. Mode shape.

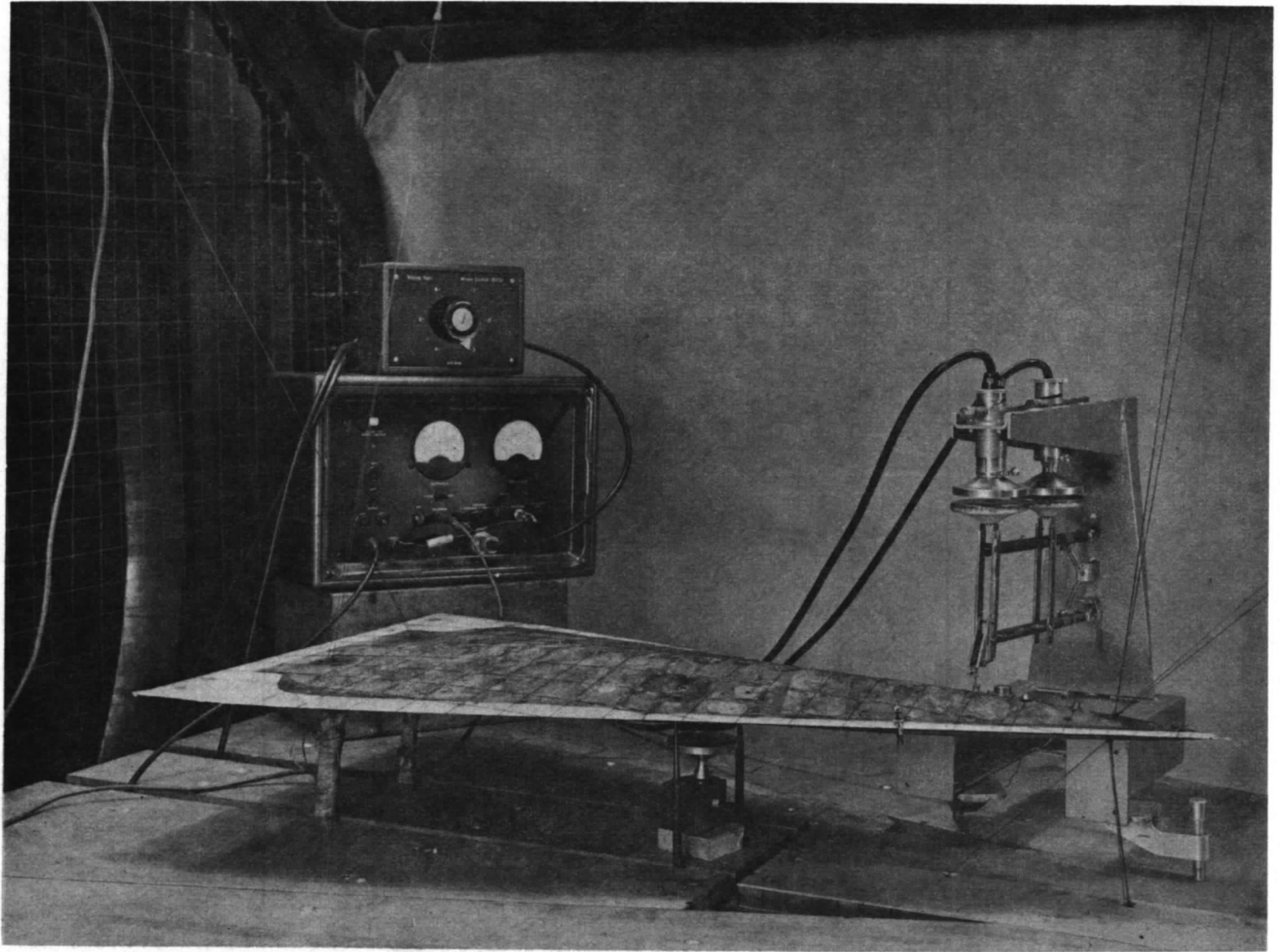
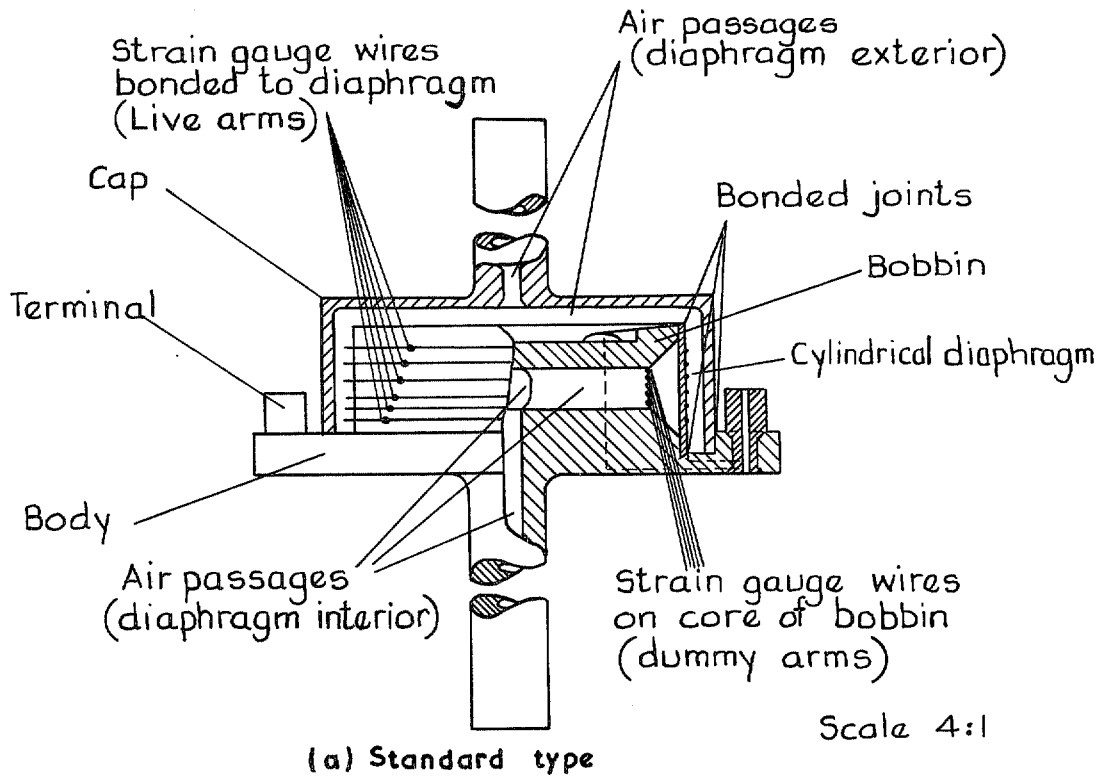


FIG. 7. Mode shape measuring equipment.



Materials

Body	Epoxy resin
Cap	Epoxy resin
Diaphragm	Pauls colotomy tubing
Gauge wire	0.00055 in dia Karma resistance wire 0.014 mm
Nominal resistance of each arm in bridge = 1020 Ω	
Adhesive	Acetone based "Titebond"

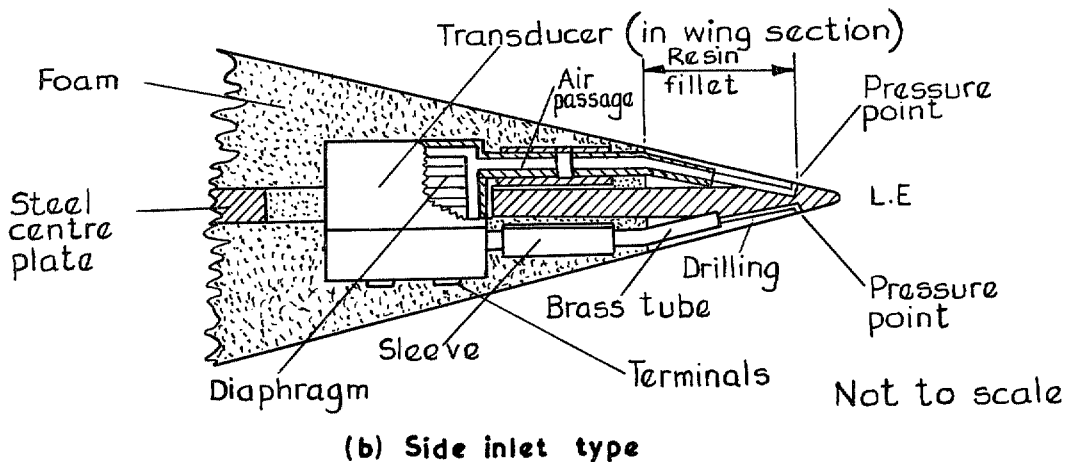


FIG. 8a and b. Sketches of pressure transducers.

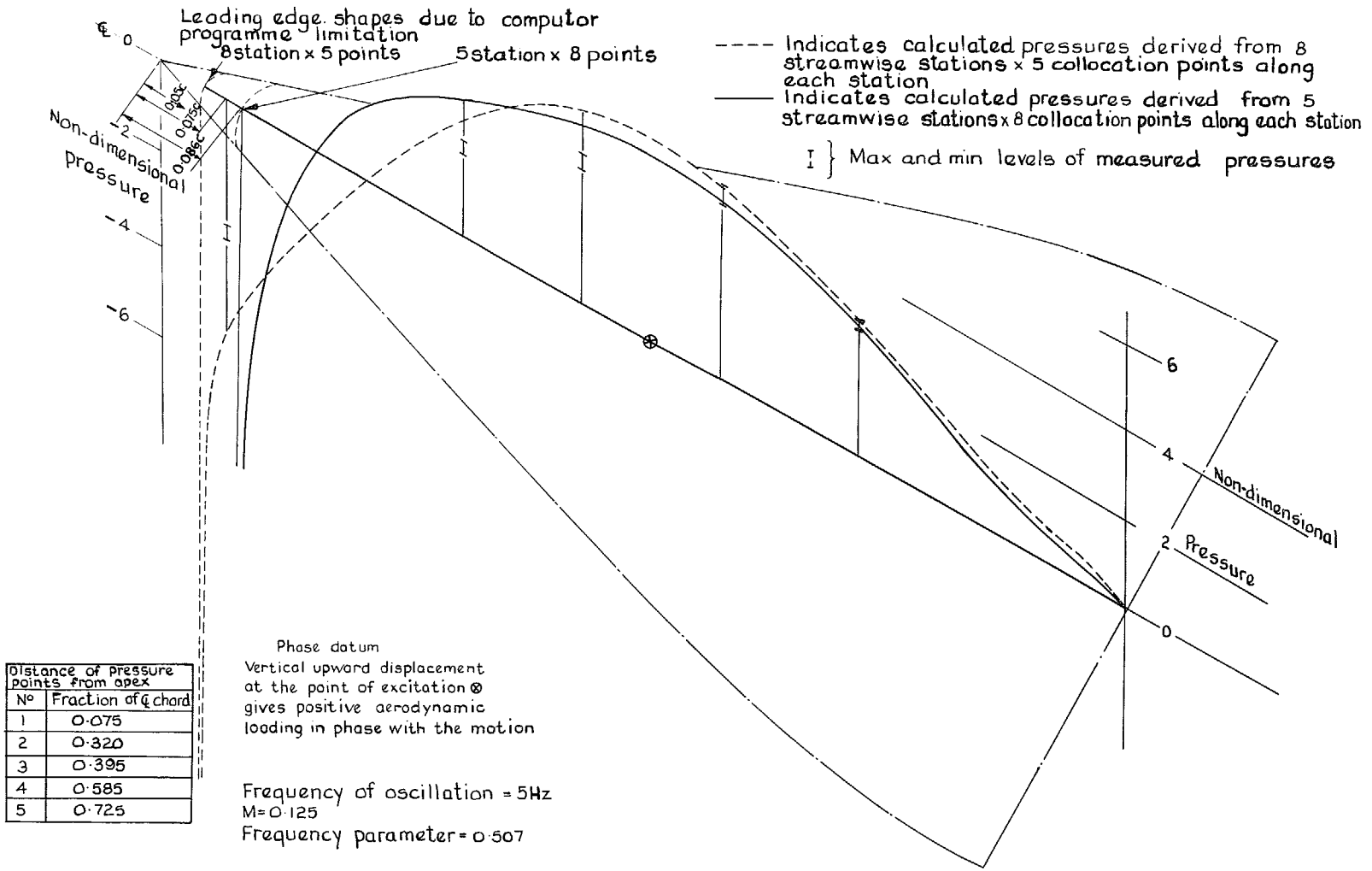


FIG. 9. In-phase pressure distribution along the centreline chord.

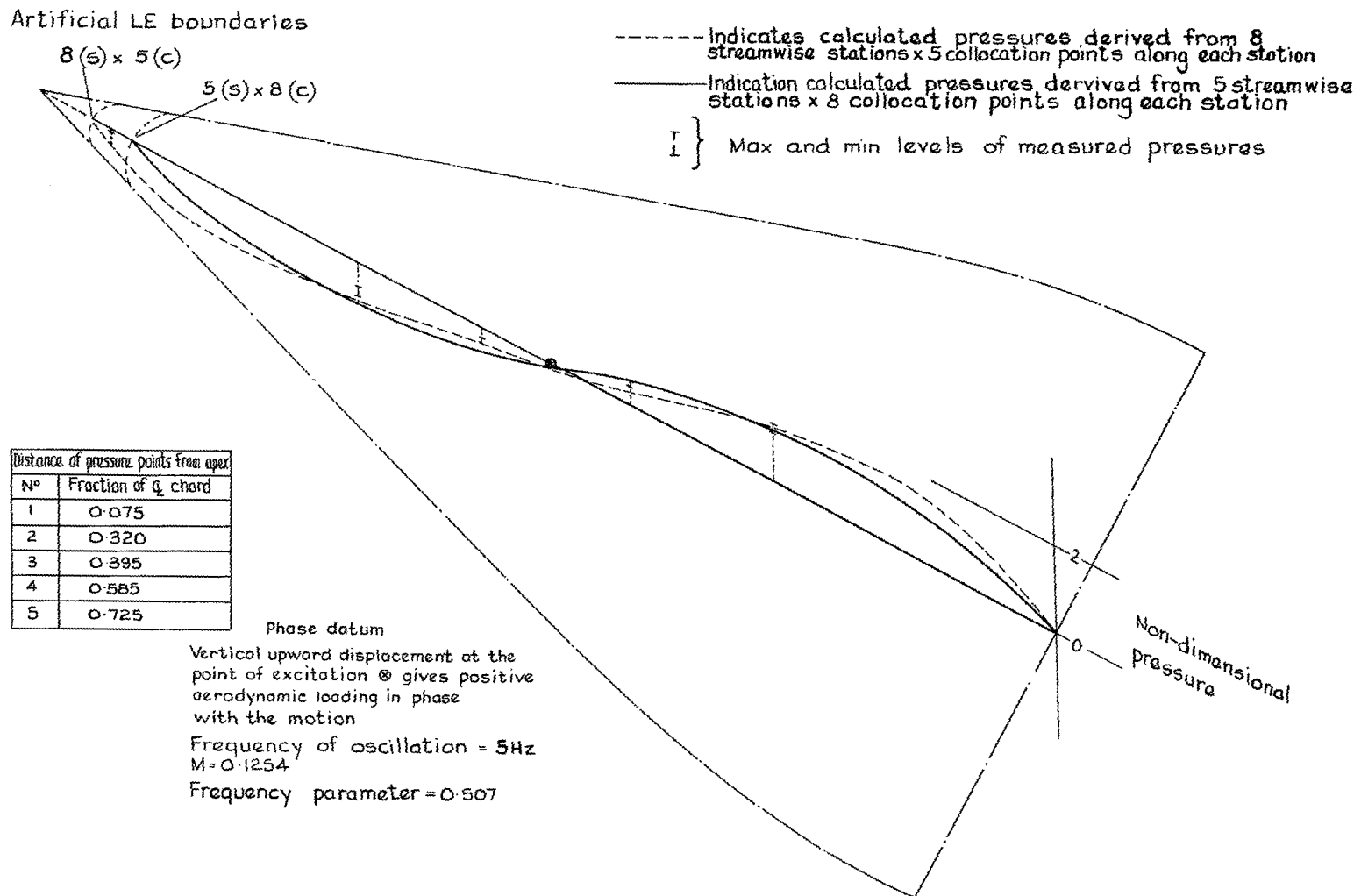


FIG. 10. In-quadrature pressure distribution along the centreline chord.

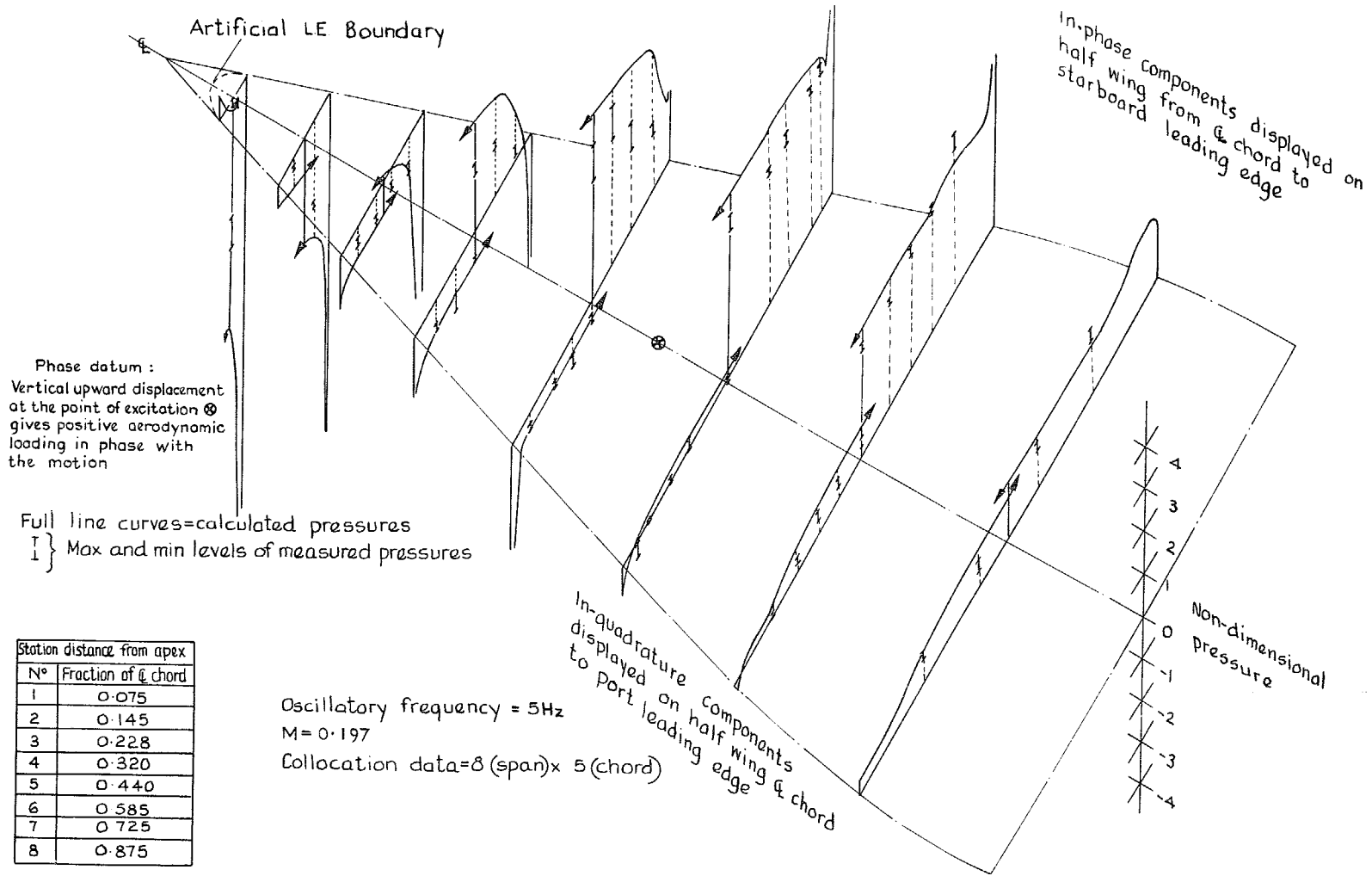


FIG. 11. Pressure distribution across the span—frequency parameter = 0.507 (derived from preferred collocation data).

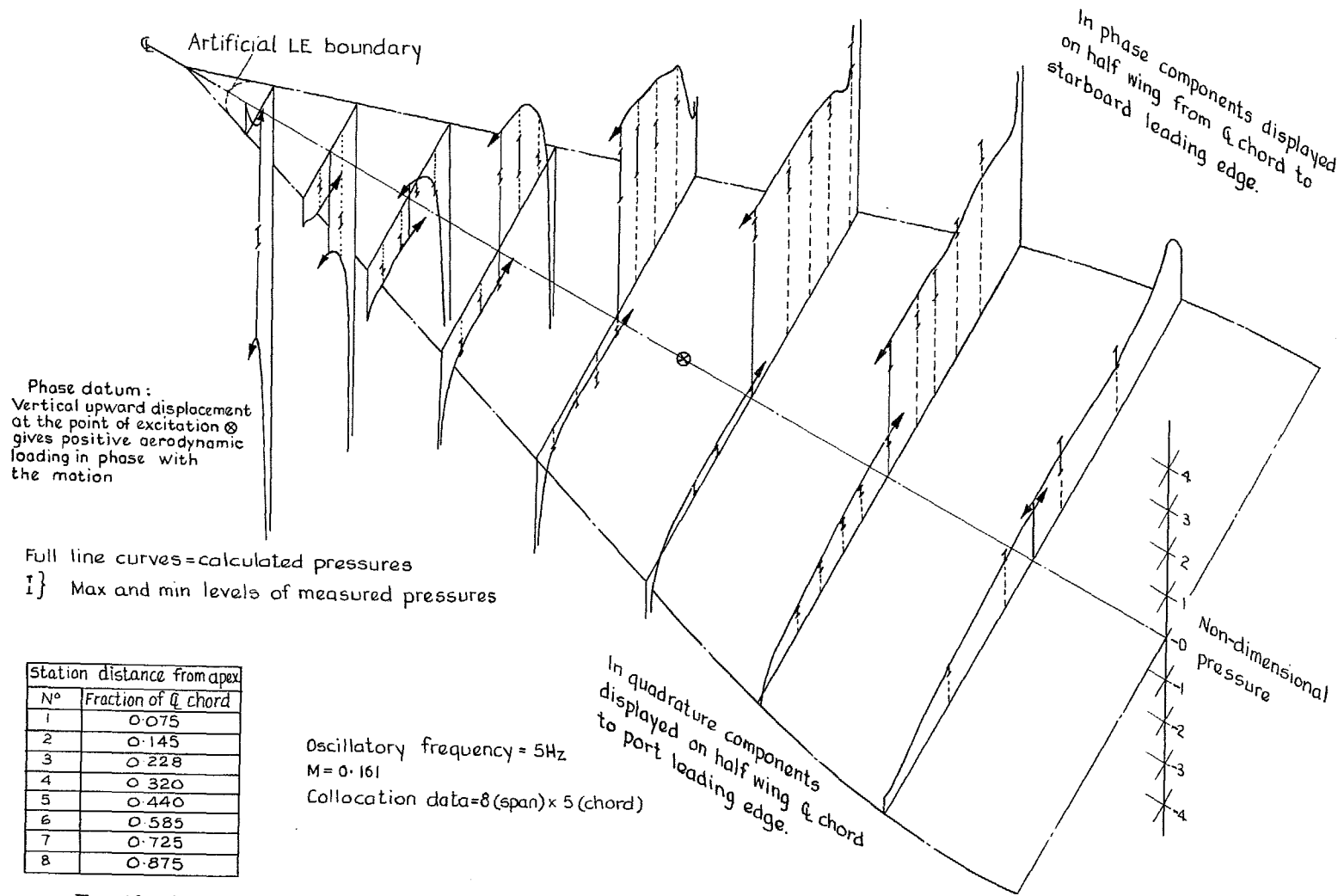


FIG. 12. Pressure distribution across the span—frequency parameter = 0.616 (derived from preferred collocation data).

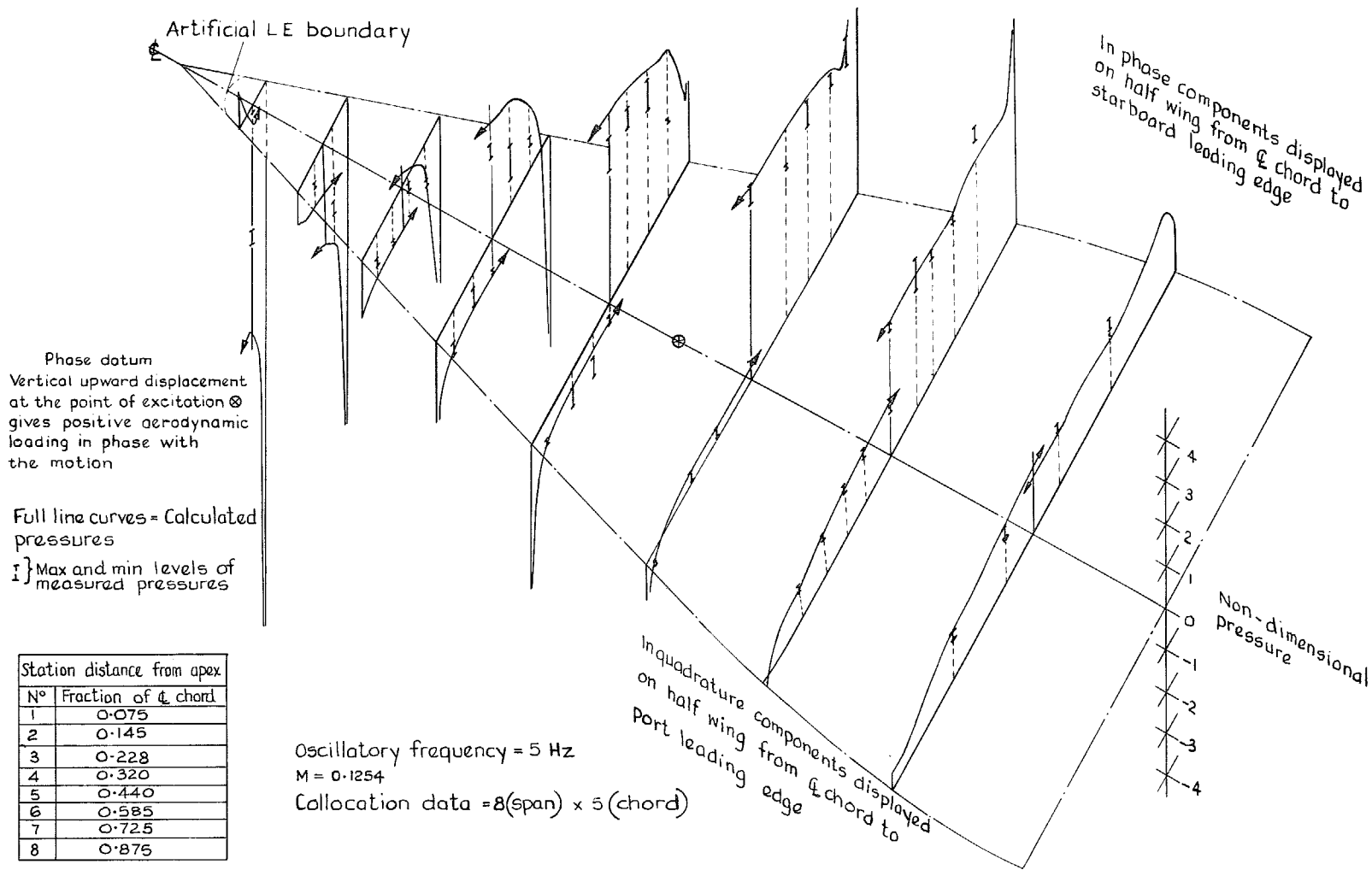


FIG. 13. Pressure distribution across the span—frequency parameter = 0.797 (derived from preferred collocation data).

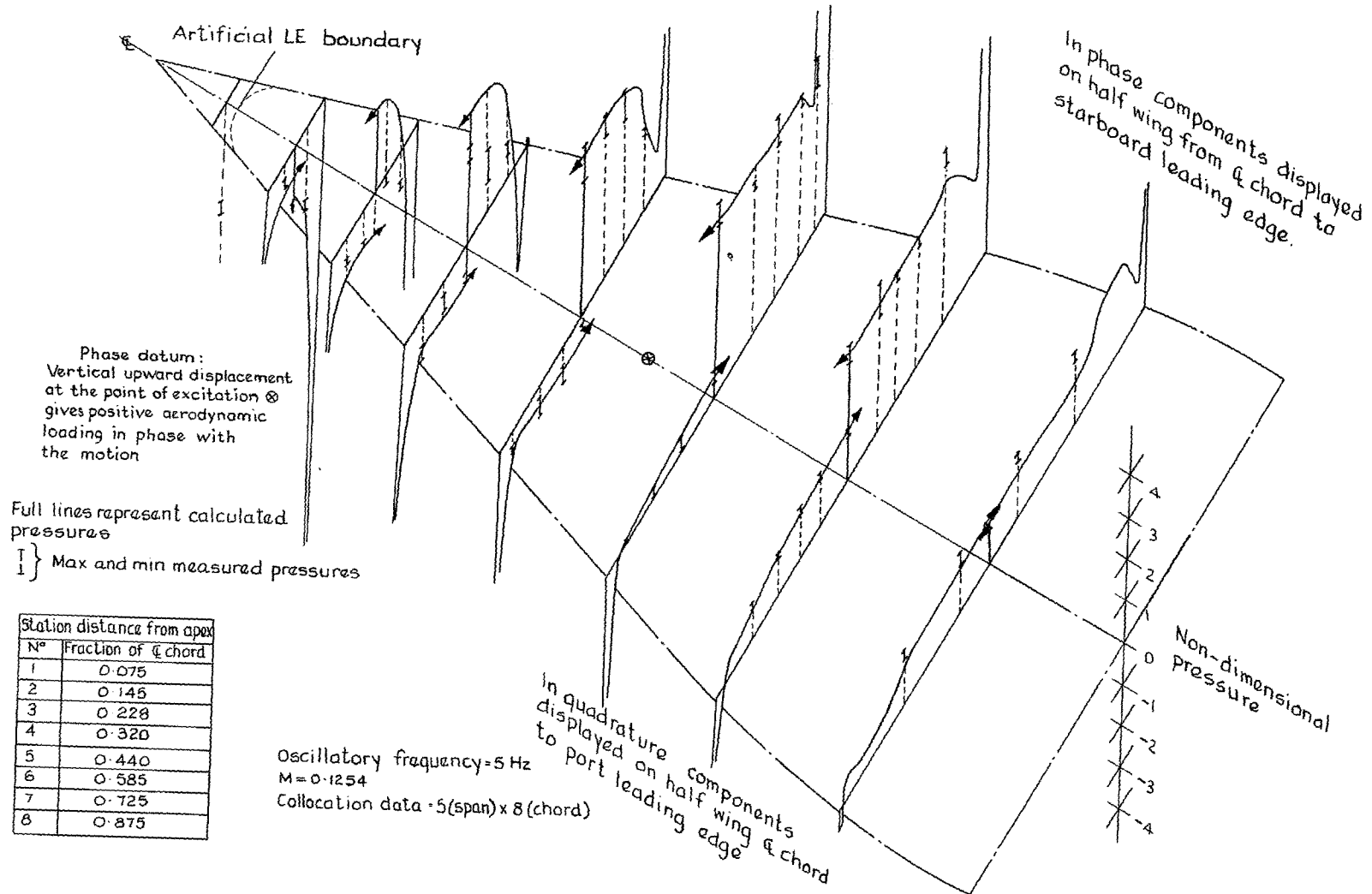


FIG. 14. Pressure distribution across the span—frequency parameter = 0.797 (derived from secondary collocation data).

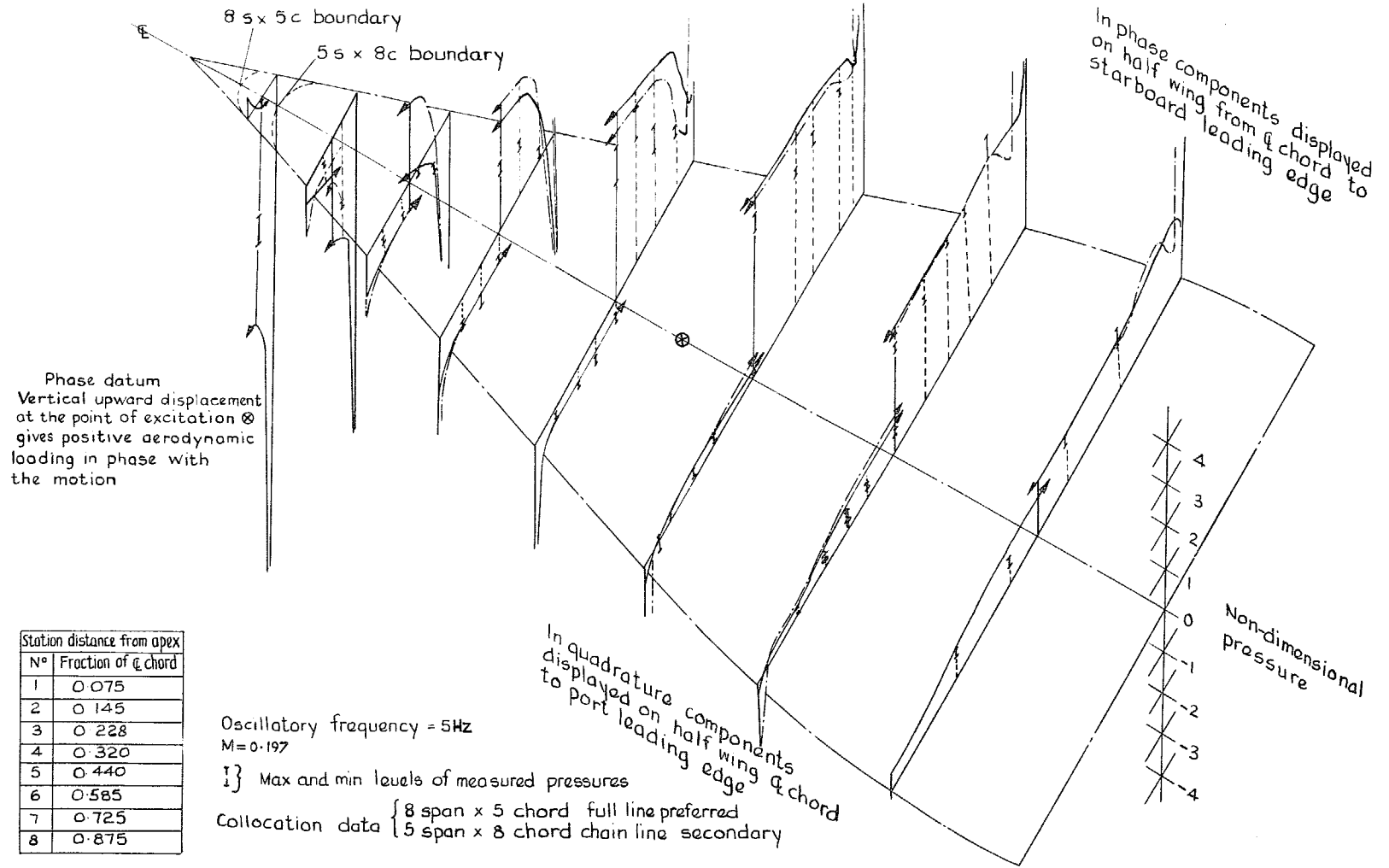


FIG. 15. Comparison of preferred with secondary calculated pressures at $M = 0.197$.

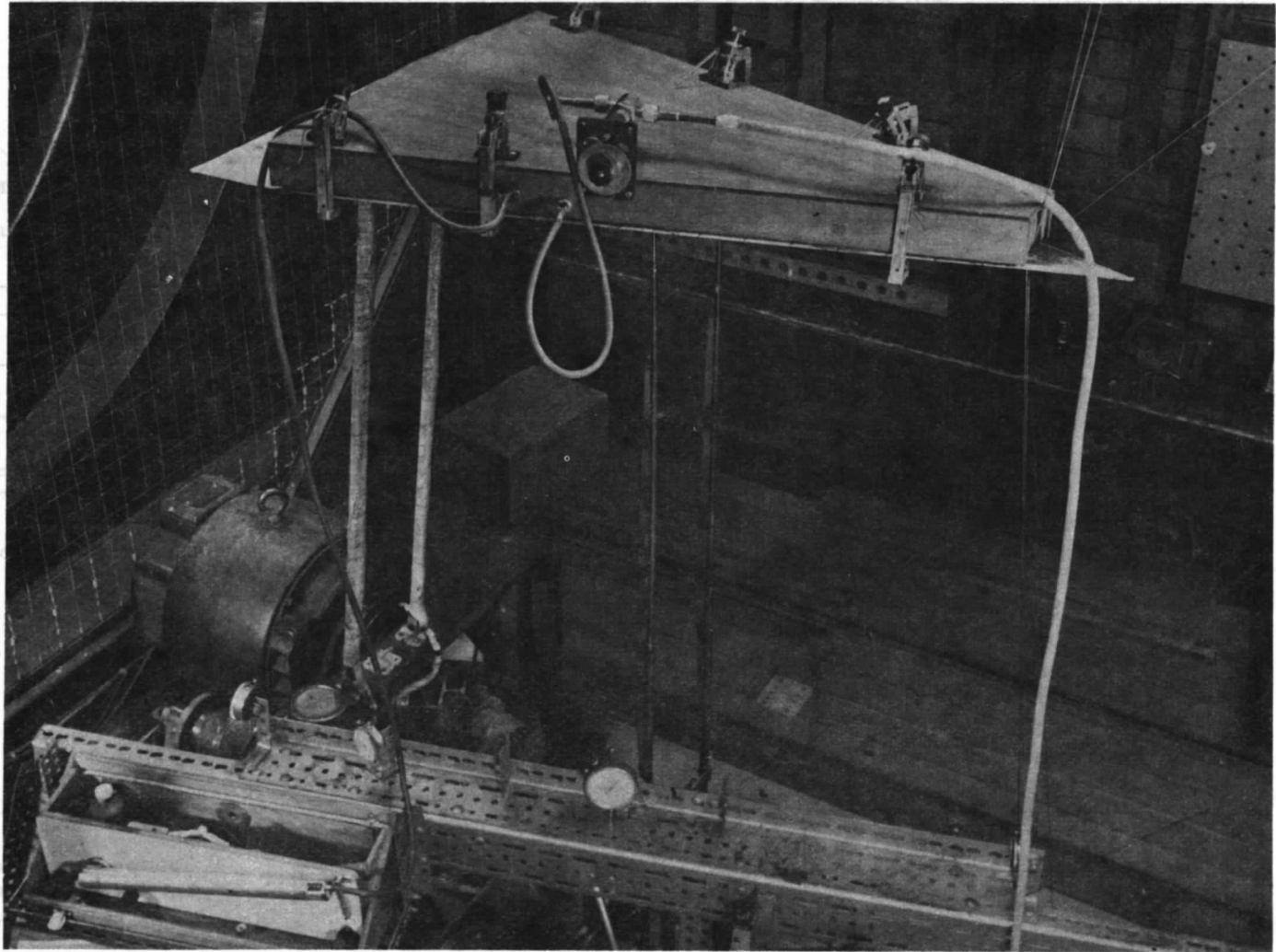


FIG. 16. Equipment used for preliminary static calibration of pressure transducers.

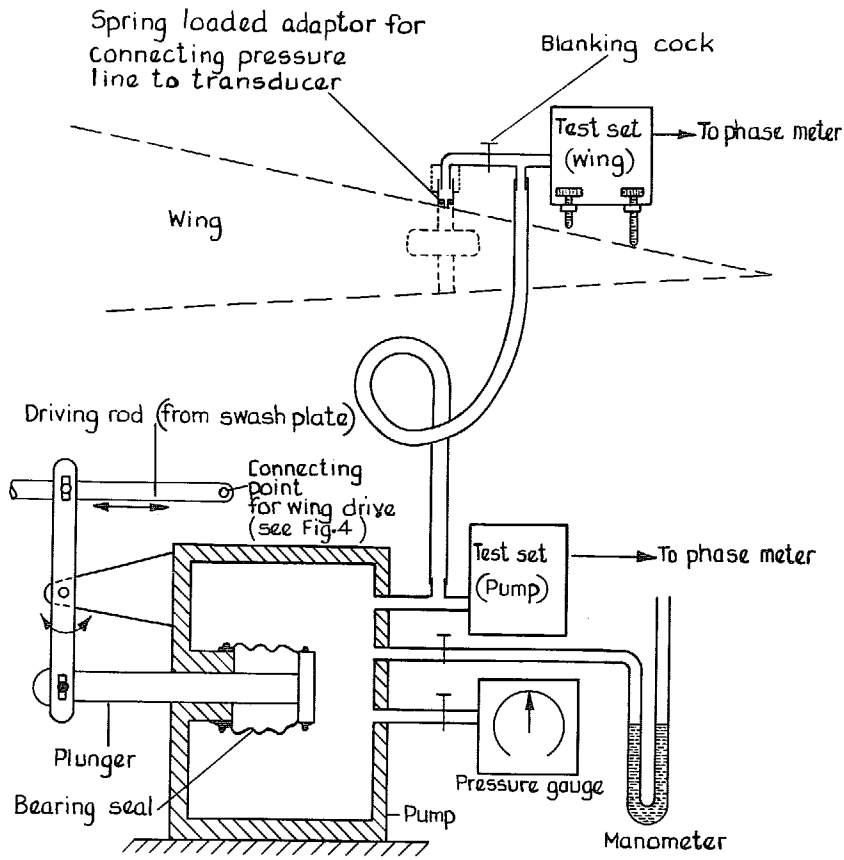


FIG. 17. Dynamic calibration equipment —diagrammatic.

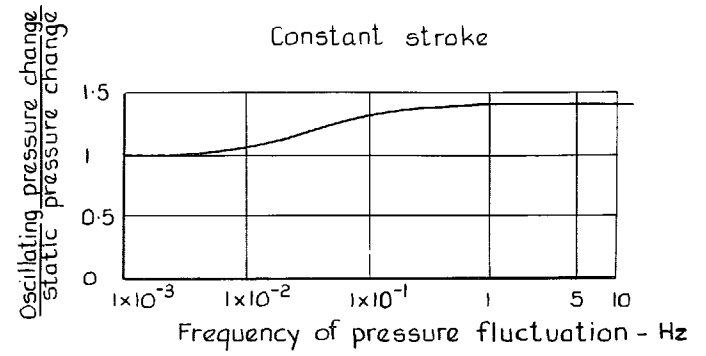


FIG. 18. Variation of pump pressure with frequency.

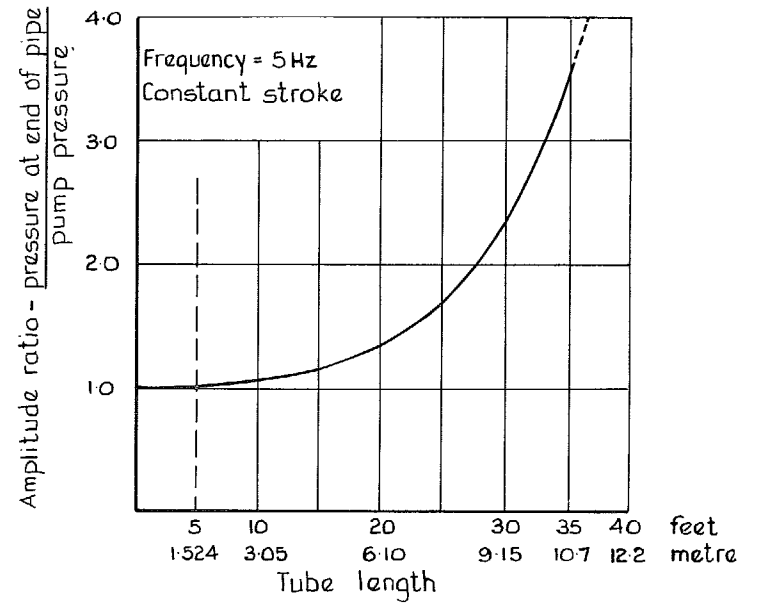


FIG. 19. Effect of tube length on pressure amplitude.

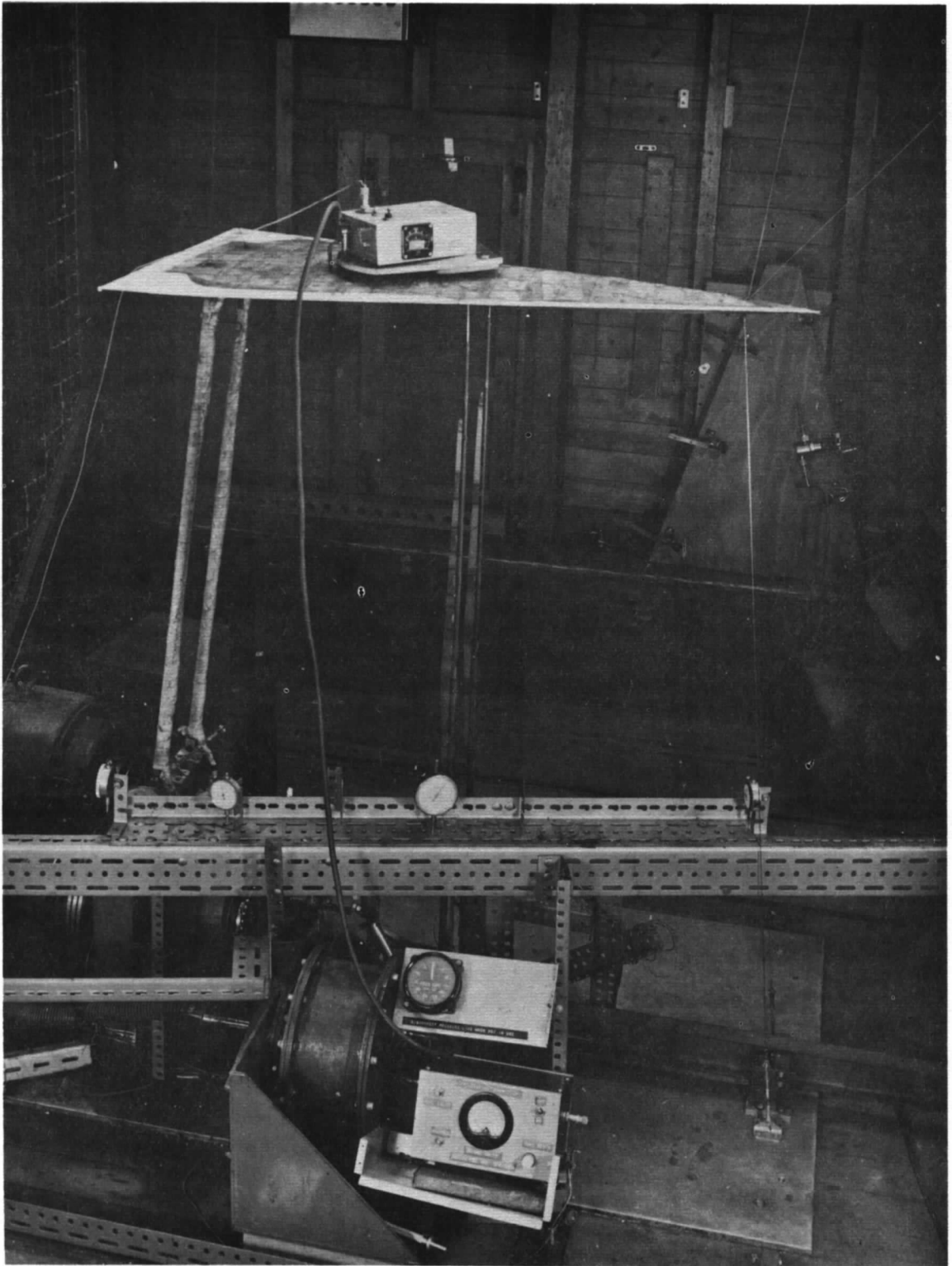


FIG. 20. Equipment used for dynamic calibration.

Printed in England for Her Majesty's Stationery Office by J. W. Arrowsmith Ltd., Bristol BS3 2NT

Dd. 135646 K.5.

© *Crown copyright 1969*

Published by
HER MAJESTY'S STATIONERY OFFICE

To be purchased from
49 High Holborn, London W.C.1
13A Castle Street, Edinburgh EH2 3AR
109 St. Mary Street, Cardiff CF1 1JW
Brazenose Street, Manchester M60 8AS
50 Fairfax Street, Bristol BS1 3DE
258 Broad Street, Birmingham 1
7 Linenhall Street, Belfast BT2 8AY
or through any bookseller